



Title	Effect of Circularly Polarized Light on Germination, Hypocotyl Elongation and Biomass Production of Arabidopsis and Lettuce; Involvement of Phytochrome B
Author(s)	LKHAMKHUU, ENKHSUKH
Citation	北海道大学. 博士(生命科学) 甲第13946号
Issue Date	2020-03-25
DOI	10.14943/doctoral.k13946
Doc URL	<a href="http://hdl.handle.net/2115/89205">http://hdl.handle.net/2115/89205</a>
Type	theses (doctoral)
File Information	LKHAMKHUU_ENKHSUKH.pdf



[Instructions for use](#)

# Doctoral Dissertation

Effect of Circularly Polarized Light on Germination, Hypocotyl  
Elongation and Biomass Production of Arabidopsis and Lettuce;  
Involvement of Phytochrome B

(植物における左右円偏光の発芽・胚軸伸長・成長に与え  
る影響に関する研究)

Lkhamkhuu Enkhsukh

Graduate School of Life Science, Hokkaido University

2020. 3

Table of contents

Abbreviations

Chapter 1. Introduction

1.1 General introduction.....1-3

1.2 The outline of this dissertation.....4

1.3 References.....5-6

Chapter 2. Germination

2.1 Introduction.....7-9

2.2 Experiments.....10-13

2.3 Results and discussions.....14-15

2.4 References.....16

Chapter 3. Hypocotyl elongation

3.1 Introduction.....17-20

3.2 Experiments.....21

3.3 Results and discussions.....22-24

3.4 References.....25

## Chapter 4. Biomass

4.1 Introduction.....	26-28
4.2 Experiments.....	29-30
4.3 Results and discussions.....	30-33
4.4 References.....	34-35

## Chapter 5. Circular dichroism spectroscopy

5.1 Introduction.....	36-38
5.2 Experiments.....	38-43
5.3 Results and discussions.....	44-51
5.4 References.....	52-53

Chapter 6. Concluding remarks.....	54-56
------------------------------------	-------

Aknowledgements.....	57
----------------------	----

## Abbreviations

At	Arabidopsis thaliana
CD	circular dichroism
CPL	circular polarized light
Cry	cryptochrome
FMN	flavin mononucleotide
LOV	light, oxygen voltage-sensing domain
LPL	linearly polarized light
L-CPL	left-handed circular polarized light
PCB	phycocyanobilin
Pfr	far-red light-absorbing form
Phot	phototropin
Phy	phytochrome
phyA	phytochrome A
phyB	phytochrome B
Pr	red light-absorbing form
P $\square$ B	phytochromobilin
R-CPL	right-handed circular polarized light
UV	ultraviolet
Vis	visible

## **Chapter 1.**

### **General introduction**

## 1.1 General Introduction

Light, especially sunlight, is a fundamental energy source. Plants utilize sunlight to synthesize carbohydrates through the process of photosynthesis. Most natural light is unpolarized, as it consists of mixtures of randomly polarized light, whereas polarized light, such as linearly polarized light (LPL) and circularly polarized light (CPL) can be generated artificially by polarizers. Polarized light is useful for spectroscopic studies analyzing the structure of chiral materials<sup>1</sup>. The plane of LPL is rotated to the left or right by passing through chiral materials, such as amino acids and carbohydrates, depending on their chirality, also known as optical activity<sup>2</sup>.

The differential absorption of left- (L-CPL) and right- (R-CPL) CPL is defined as circular dichroism<sup>3</sup> (CD). These spectroscopic features provide essential information to determine the stereochemical structures of these compounds, including their absolute configurations, which are difficult to determine by other methods. To date, most chiroptical spectroscopic studies have been performed at the molecular level<sup>4</sup>. Many biopolymers in organisms contain optically active molecules, such as L-amino acids and D-glucose, which absorb L-CPL and R-CPL unequally. CD is an established spectroscopic method used to analyze the secondary structure of proteins<sup>5</sup> and DNA<sup>5</sup>. Furthermore, complexes of biopolymers, such as arthropod cuticles, plant cell walls and human compact bone osteon, form cholesteric liquid crystals and scatter CPL<sup>6</sup>. Studies have suggested that communications in the scarab beetle *Chrysina gloriosa* involve CPL reflection<sup>7</sup>, and several types of crustaceans, including stomatopods<sup>8</sup>, sapphirinidae copepods<sup>9</sup> and mantis shrimp<sup>10</sup>, have been reported to recognize CPL. Plant tissues that reflect CPL include *Pollia* fruit<sup>11</sup>, leaves of the herb *Mapania caudate*<sup>12</sup> and starch granules from *Solanum tuberosum*<sup>13</sup>. CPL reflection has also been used to analyze the fibrillar structure of bone<sup>14</sup>.

In plants, granal chloroplasts show CD in a red light-absorbing region of chlorophyll, with circularly polarized chlorophyll luminescence used to measure chiral macroaggregates of light-harvesting chlorophyll-protein complexes in chloroplasts<sup>15</sup>. CPL was also shown to have net photosynthetic activity and to be involved in the synthesis of chlorophyll in the unicellular marine flagellate, *Dunaliella euchlora*. R-CPL showed greater activity than L-CPL, suggesting that the receptor pigments responsible for these phenomena sense CD<sup>16</sup>. To date, however, only one study has reported that CPL had a differential effect on plant growth. In that study, L-CPL induced faster growth of the shoots of lentil and pea plants than R-CPL although the CPL did

not change significantly after penetration through the outer layer cells of leaves and stems<sup>17</sup>. Thus, the effect of CPL on plant growth is poorly understood.

In addition to photosynthesis, physiological responses of plants to light are regulated by photoreceptors. Immobile, photosynthetic plants must adapt precisely to their environmental conditions, including light. Plants have various photoreceptors that receive light signals over a wide spectrum, ranging far-red to ultraviolet B light<sup>18</sup>. These receptors include phytochrome; two blue light receptors, cryptochrome (cry) and phototropin (phot); and UV-B resistance 8 (UVR-8).

Phytochrome B (phyB) is a photochromic receptor interconvertible between its red light-absorbing form (Pr) and its far-red light-absorbing form (Pfr) following exposure to red and far-red light, respectively<sup>19</sup>. Phytochrome B (phyB) has been reported to regulate the germination<sup>20</sup> and hypocotyl elongation<sup>21</sup> of Arabidopsis, suggesting that differences in the responses of these plants to R- and L-CPL may be due to the chiral structure of phyB and its different photoreaction to R- and L-CPL.

The present study evaluated the effects of CPL on the growth of Arabidopsis and lettuce plants, including effects on germination, hypocotyl elongation and biomass production. To determine the molecular basis of CPL perception, the CD spectrum and the effect of CPL on photoconversion were measured with the sensory module of Arabidopsis phyB, which binds phycocyanobilin (PCB) rather than the native chromophore phytylchromobilin (PΦB). These findings showed that phyB, along with other photoreceptors and photosynthesis, is involved in the effects of CPL on plant physiological responses.



## **1.2 The outline of this dissertation**

In chapter 2 shows L-CPL and R-CPL have different effects on the germination of Arabidopsis and lettuce seeds. Depending on red light intensity and duration of light illumination studies by circular polarized lights for indicating that the Phy B molecules responsible for the seed germination are able to sense the chirality of red light.

In chapter 3 hypocotyl elongation of two different species of photoinhibition by L-CPL and R-CPL and their hypocotyl lengths were quantified using ImageJ computer software. Photoinhibition of hypocotyl elongation of red light perception compared with wild type of seed and mutant type of seeds described.

In chapter 4, effects of white circular polarized lights on biomass production by Arabidopsis, with biomass is defined as the average fresh weight of an above-ground part of an adult plant, found that the average tissue weights L- and R-CPL. To assess the effects of light, Arabidopsis was cultured under red, green or blue CPL, although the total fluence of these CPLs differed.

Chapter 5 shows determination of involvement of phyB in the observed effects of CPL, UV-visible (UV-Vis) absorption spectra of a PCB-bound sensory module of Arabidopsis phyB, AtphyB-N651, were measured in Pr and a photostationary state between Pr and Pfr induced by saturating with red light illumination

## References

1. Li, W.; Coppens, Z. J.; Besteiro, L. V.; Wang, W.; Govorov, A. O.; Valentine, J. *Nat Commun*, **2015**, 6, 8379
2. Bromage, T. G.; Goldman, H. M.; McFarlin, S. C.; Warshaw, J.; Boyde, A.; Riggs, C. M. *Anat Rec B New Anat*, **2003**, 274, 157-168.
3. Polavarapu, P. L. *Chirality*, **2002**, 14, 768-781.
4. Harada, N.; Nakanishi, K.; Berova, N. *Principles and Applications in Comprehensive Chiroptical Spectroscopy* (ed. Berova, N., Polavarapu, P. L., Nakanishi, K. & Woody, R. W.), **2012**, 115-166 (John Willey & Sons, Inc.)
5. A) Vorlíčková, M.; Kejnovská, I.; Bednářová, K.; Renčíuk, D.; Kypr, J. *Chirality*, **2012** 24, 691-698.  
B) Whitmore, L.; Wallace, B. A. *Biopolymers*, **2008**, 89, 392-400.
6. Mitov, M.; Dessaud, N. *Nat Mater*, **2006**, 5, 361-364.
7. Brady, P.; Cummings, M. *Am Nat*, **2010**, 175, 614-620.
8. Chiou, T. H.; Kleinlogel, S.; Cronin, T.; Caldwell, R.; Loeffler, B.; Siddiqi, A.; Goldizen, A.; Marshall, J. *Curr Biol*, **2008** 18, 429-434.
9. Baar, Y.; Rosen, J.; Shashar, N. *PLoS One*, **2014**, 9: e86131
10. Gagnon, Y. L.; Templin, R. M.; How, M. J.; Marshall, N. J. *Curr Biol*, **2015**, 25, 3074-3078.
11. Vignolini, S.; Rudall, P. J.; Rowland, A. V.; Reed, A.; Moyroud, E.; Faden, R. B.; Baumberg, J. J.; Glover, B. J.; Steiner, U. *Proc Natl Acad Sci USA*, **2012**, 109, 15712-15715.
12. Strout, G.; Russell, S. D.; Pulsifer, D. P.; Erten, S.; Lakhtakia, A.; Lee, D. W. *Ann Bot*, **2013**, 112, 1141-1148.
13. Zhuo, G. Y.; Lee, H.; Hsu, K. J.; Huttunen, M. J.; Kauranen, M.; Lin, Y. Y.; Chu, S. W. *J Microsc*, **2014**, 253, 183-190.
14. Spiesz, E. M.; Kaminsky, W.; Zysset, P. K. *J Struct Biol*, **2011**, 176, 302-306.
15. Hall, J.; Renger, T.; Picorel, R.; Krausz, E. *Biochim Biophys Acta*, **2016**, 1857, 115-128.
16. McLeod, G. C. *Limnol Oceanogr*, **1957**, 2, 360-362.
17. Shibayev, P. C.; Pergolizzi, R. G. *Int J Botany*, **2011**, 7, 113-117.
18. Paik, I.; Huq, E. *Semin Cell Dev Biol*, **2019**, 92, 114-121.

19. Li, J.; Li, G.; Wang, H.; Wang, D. X. *Arabidopsis Book*, **2011**, 9: e0148.
20. Shinomura, T.; Nagatani, A.; Hanzawa, H.; Kubota, M.; Watanabe, M.; Furuya, M. *Proc Natl Acad Sci USA*, **1996**, 93, 8129- 8133.
21. Reed, J.W.; Nagpal, P.; Poole, D. S.; Furuya, M.; Chory, J. *Plant Cell*, **1993**, 5, 147-157.

## **Chapter 2.**

### **Germination**

## 2.1 Introduction

Light is an important environmental factor controlling plant growth and development. Not only does light provide energy for photosynthesis, but plant growth patterns and a large number of plant developmental events, such as formation of leaf primordia, plastid development, and induction of flowering, are also responsive to light cues<sup>1</sup>.

Physiological experiments suggest that two major plant regulatory photoreceptor systems are active in perception of light cues: one system sensing shorter wavelength blue and UV-A light, and the second sensing predominantly longer wavelength red/far red light<sup>2</sup>. Light responses that are known to be mediated by phytochromes include germination, chloroplast development, leaf expansion, regulation of gene expression, inhibition of cell elongation, and photoperiodic control of flowering<sup>3</sup>.

The photoinduction of seed germination examined in 1935, found that continuous irradiation with light of 580-700 nm was effective in inducing germination of lettuce seeds<sup>4</sup> (fig. 1). In 1952, reported the determination of effect of brief exposures to red and far-red light in lettuce seeds, and discovered the red/far-red photoreversible response<sup>5</sup>, that measured the action spectra for promotion and inhibition of germination, finding the maximum sensitivity for promotion in the region of 640-670 nm and that for inhibition in 720-750 nm.

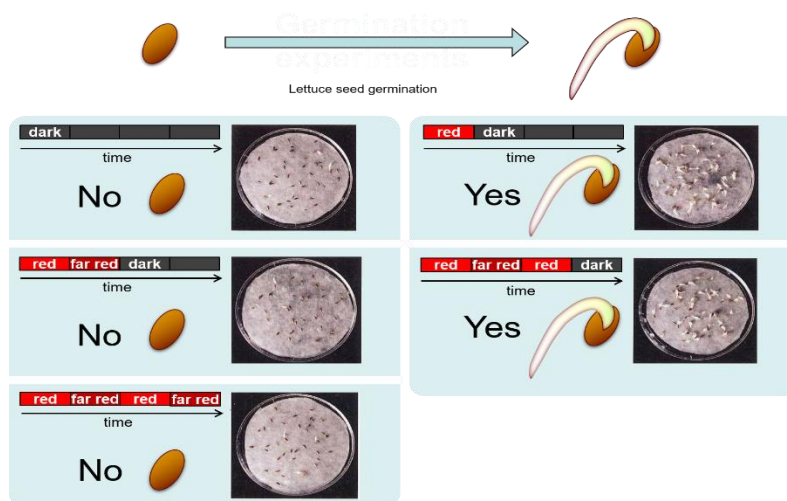


Figure 1. Lettuce seed germination is a typical photo-reversible response controlled by phytochrome. L. Taiz, E. Zeiger, *Plant physiology, fifth edition, Sinauer Associates, Inc., 495 (2010)*

Very similar action spectra for photoreversible regulation of seed germination were determined in *Arabidopsis thaliana* of the wild-type<sup>6</sup> (wt) and long-hypocotyl mutants<sup>7</sup>. Shinomura report, using the *Arabidopsis* phyA and phyB mutants, that red/far-red reversible induction of seed germination is principally regulated by PhyB, but not by PhyA, and that the phyB mutant seeds became sensitive to red light after dark incubation for 48 hr, then clearly demonstrated that PhyA photoirreversibly triggers the germination upon irradiations with ultraviolet, visible and farred light of very low fluence, while PhyB controls the photoreversible effects of low fluence<sup>8</sup> (fig. 2).

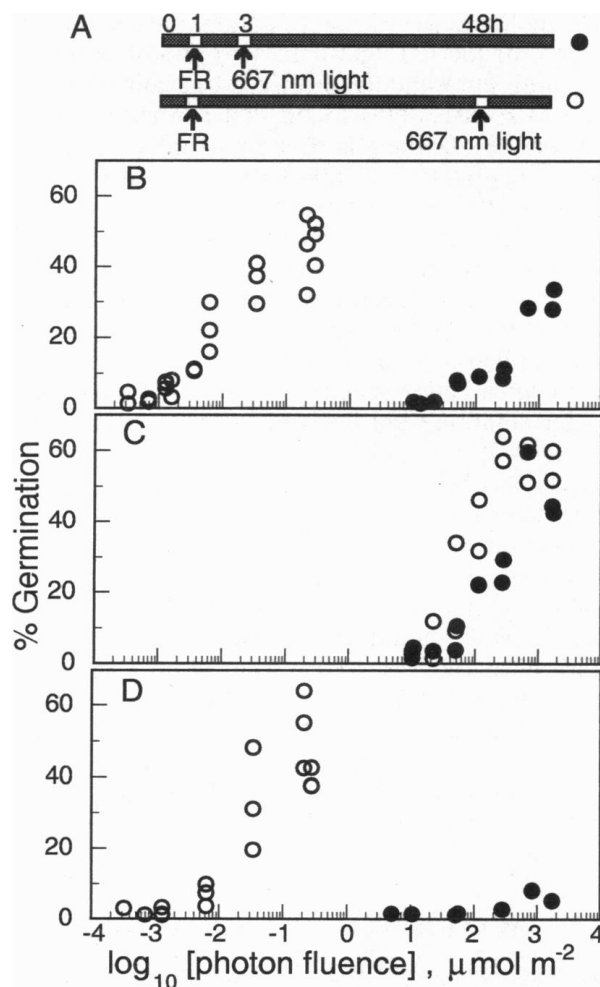


Figure 2. Effects of incubation time and photon fluence of red light on seed germination. (A) Light regime of the experiment. Black bars, incubation period on aqueous agar plates in darkness at 25 + 1°C white bars with arrows, pretreatments with far-red light (FR) and exposures to 667 nm light; 0 and 0, germination rates of seeds that were kept in darkness for 3 and 48 hr, respectively. (B-D) Fluence response relationships for the wt (B), the phyA mutant (C), and the phyB mutant (D) seeds.

## 2.2 Experimental section

### 2.2.1 Materials

#### *Plant materials*

Seeds of *Arabidopsis* (*Arabidopsis thaliana*: *At*) wild type (ecotype Columbia-0) were the kind gifts of Prof. Akira Nagatani at Kyoto University. Lettuce seeds (*Lactuca sativa* L.) were purchased from Sakata Seed Corporation (Yokohama, Japan). Surface-sterilized seeds were placed on filter paper soaked with water or Murashige and Skoog (MS) medium supplemented with 2% (W/V) sucrose (Germination Inducible Medium: GIM) in a Petri dish. The seeds were incubated in the dark at 4°C for 48 h to synchronize germination. The detailed growth conditions are shown in each section.

### 2.2.2 General methods, Instrumentation and measurements

#### *Germination assay*

*Arabidopsis* seeds (60–200 grains) were placed on water-soaked filter paper in Petri dishes. After incubation at 4°C for 48 h in the dark, the seeds were irradiated with red L- or R-CPL (1.02  $\mu\text{mol}/\text{m}^2/\text{s}$ ) for 10 min at 22°C and kept in the dark for 3 days at 22°C. Lettuce seeds were treated similarly, except that the intensity of irradiated light was 0.36  $\mu\text{mol}/\text{m}^2/\text{s}$ . Germinated seeds were counted, and germination rates were calculated and compared by Student's t-tests (fig. 3).

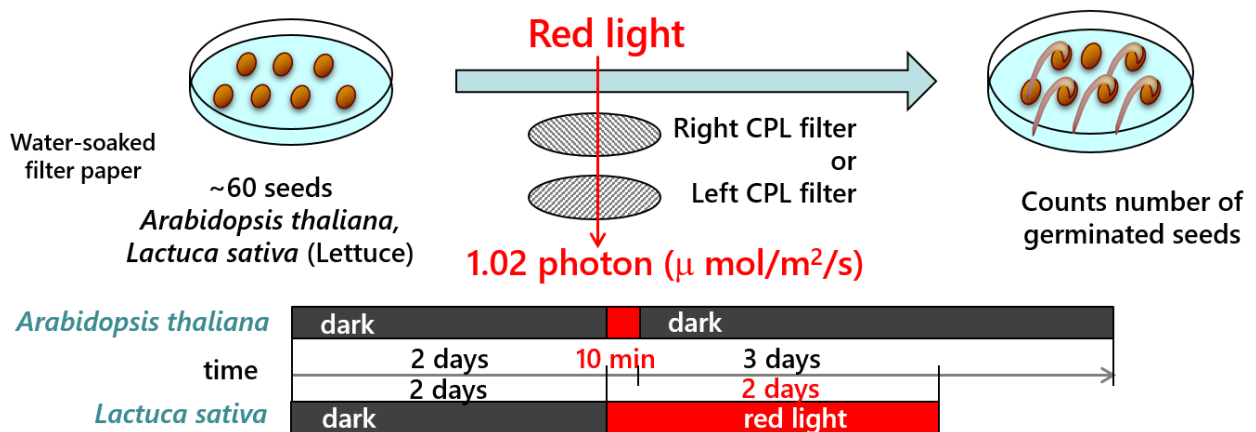


Figure 3. germination experimental scheme.

### ***Light condition in growth chamber***

Plants were cultured in LED plant growth chambers (LH-70LED-DT, Nippon Medical & Chemical Instruments Co., Ltd., Japan), containing three monochromatic LEDs (red LED,  $\lambda_{\text{max}} = 660 \text{ nm}$ ; green LED,  $\lambda_{\text{max}} = 525 \text{ nm}$ ; and blue, LED  $\lambda_{\text{max}} = 450 \text{ nm}$ ). CPL was generated by filtering the LED light through circularly polarizing filters (Polarization Control Film, Fujifilm Corporation, Japan). Each filter consisted of a linear polarization plate and a quarter wavelength plate (fig. 3). The chiroptical purity of L- and R-CPL was examined by a Haze meter (NDH2000, Nippon Denshoku Industries Co., LTD., Japan) (fig. 6); negligible differences in intensity and purity were observed between L- and R-CPL. The inner walls of the chamber were covered with black paper to avoid reflection of light (fig. 4). In this study, the term “white light” indicates the mixture of red, green and blue light supplied by the three LEDs in the growth chamber. Monochromatic light was generated by turning on only the red, green or blue LED. The humidity of the chamber was set at 50%.





LED weather machine LH-70LED-DT



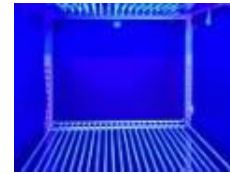
Inner side filled by black paper



photon: 10.8  
( $\mu\text{mol}/\text{m}^2/\text{s}$ )



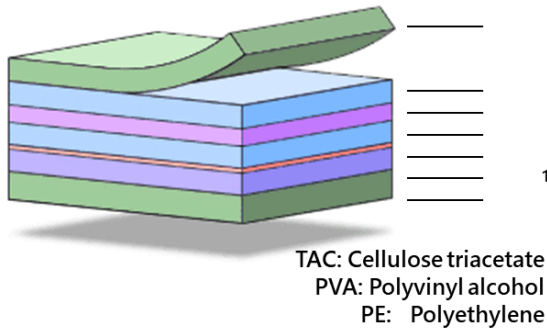
photon: 0.05  
( $\mu\text{mol}/\text{m}^2/\text{s}$ )



photon: 0.02  
( $\mu\text{mol}/\text{m}^2/\text{s}$ )

Figure 4. artificial LED weather machine LH-70LED-DT.

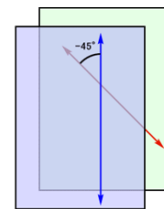
### Linear polarized film



### Circular polarized film

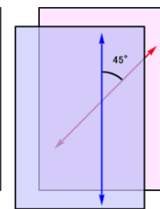
Front side: linear polarizer  
back side: 1/4 lambda film

#### Left Circular type



1/4 lambda film  
retardation axis  $-45^\circ$   
against absorbing axis  
of linear polarized film

#### Right Circular type



1/4 lambda film  
retardation axis  $+45^\circ$   
against absorbing axis  
of linear polarized film

Figure 5. simple method to create CPL for plant cultivation

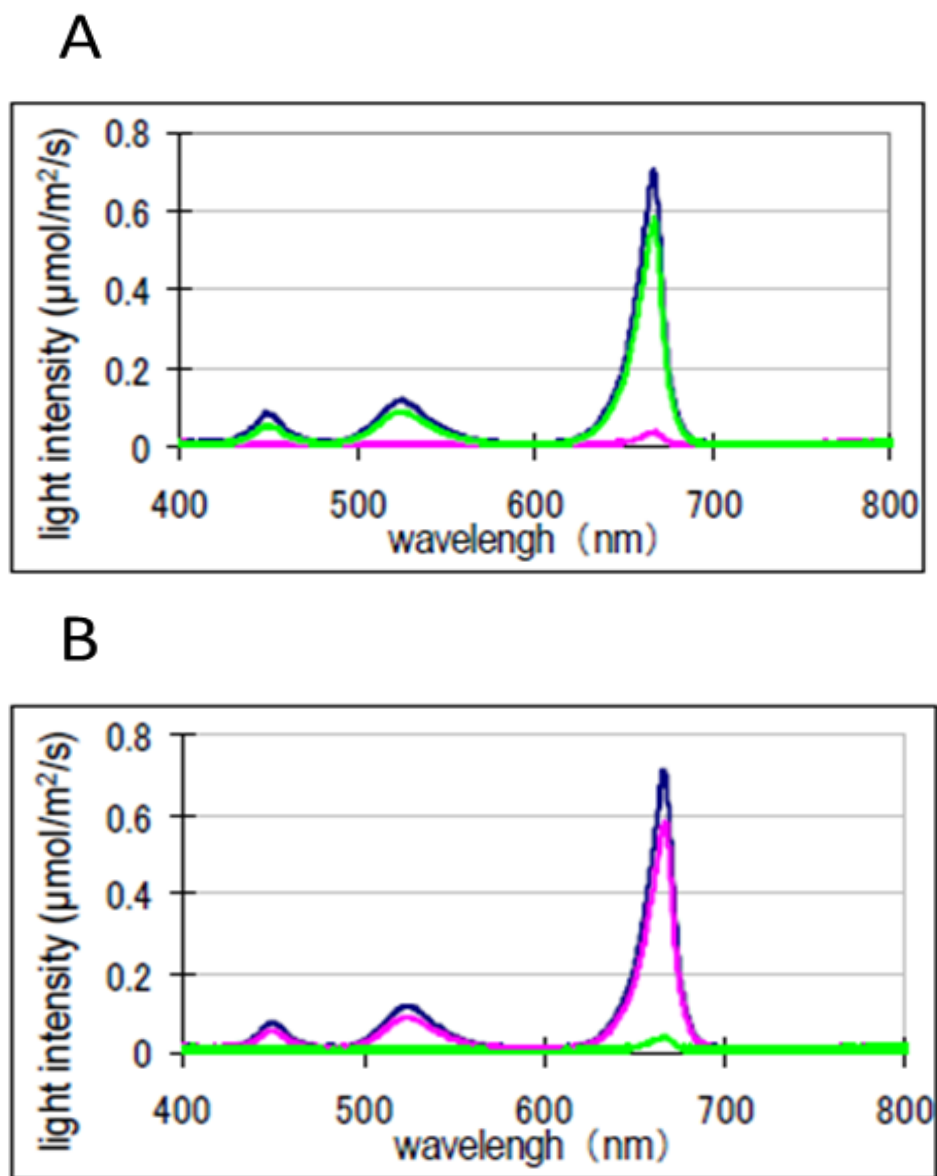


Figure 6. Emission spectra of LED light in the growth chamber with a R-CPL (A) and L-CPL (B) polarizing filters. The spectra indicate R-CPL (green), L-CPL (purple) and total light (dark blue).

### 4.3 Results and discussions

#### *Effect of red CPL on germination of Arabidopsis and lettuce seeds*

To our knowledge, this study is the first to show that L-CPL and R-CPL have different effects on the germination of Arabidopsis and lettuce seeds. The germination rates of Arabidopsis seeds in the presence of L- and R-CPL were 58.4% and 68.2%, respectively, indicating that R-CPL was more effective than L-CPL in the red light-absorbing region (Figure 7A).

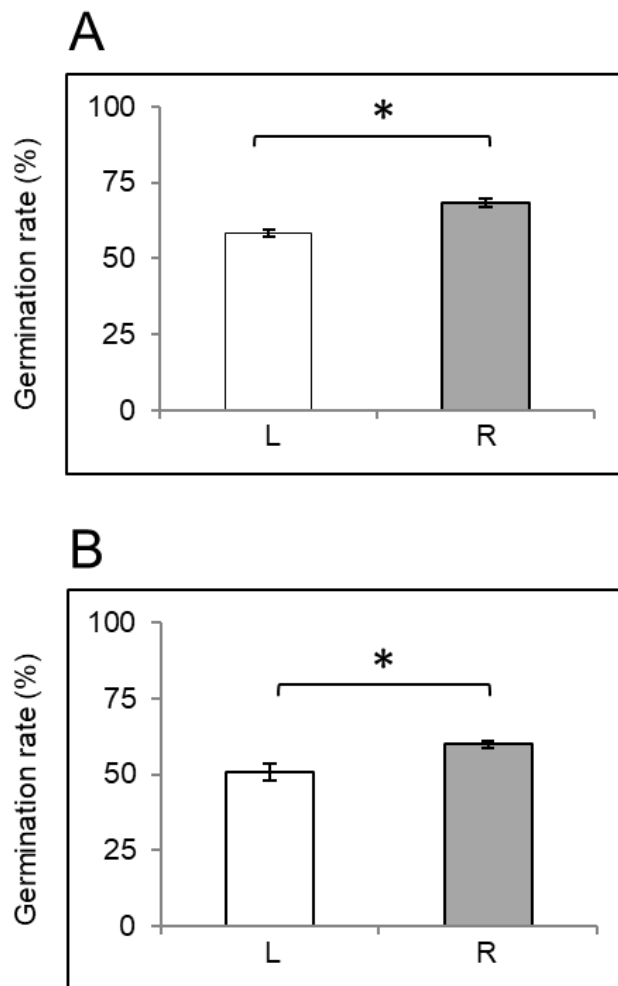


Figure 7. Effect of red CPL on germination of Arabidopsis (A) and Lettuce (B).

Cold-treated seeds were irradiated with red L- or R-CPL (L or R, respectively) for 10 min at 1.02  $\mu\text{mol}/\text{m}^2/\text{s}$  (A) and 0.36  $\mu\text{mol}/\text{m}^2/\text{s}$  (B) at 22°C. After 3 days incubation in the dark at 22°C, germinated seeds was counted and germination rate was calculated. \**t*-test  $P < 0.05$  (left and right), error bar =

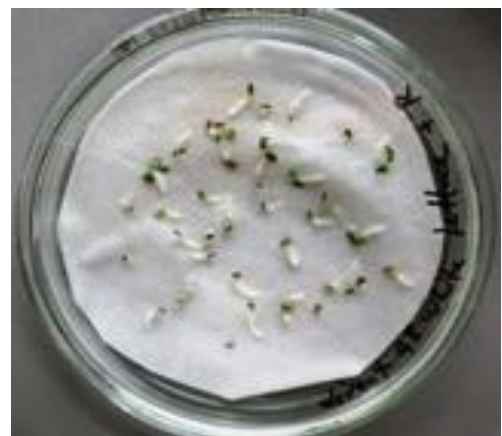
*S.D., n = 10.*

Similarly, the germination rates of lettuce seeds in the presence of L- and R-CPL were 50.7% and 59.9%, respectively (Figure 1B). Calculations showed that the germination rates of Arabidopsis and lettuce were 1.17- and 1.18-fold greater, respectively under R- than L-CPL.

Light-induced germination of Arabidopsis seeds has been reported mediated by phyA and phyB, depending on the intensity and duration of light illumination. PhyA mediates seed germination induced by red light of intensity 1–100 nmol/m<sup>2</sup>/s and far-red light of intensity 0.5–10 μmol/m<sup>2</sup>/s, both applied after incubation in the dark for 48 h. Red light-induced germination could not be reversed by subsequent far-red light illumination<sup>8</sup>, a phenomenon called the very low fluence response<sup>9</sup> (VLFR). In contrast, phyB mediates seed germination induced only by red light of intensity 10–1,000 μmol/m<sup>2</sup>/s applied after incubation in the dark for 3 h and could be reversed by subsequent illumination with far-red light<sup>8</sup>, a phenomenon called the low fluence response<sup>10</sup> (LFR). Based on the intensity and timing of the light illumination, germination in the present study corresponds to LFR mediated by phyB. The germination rates of Arabidopsis and lettuce induced by red R-CPL were greater than those induced by L-CPL, indicating that the phyB molecules responsible for the seed germination are able to sense the chirality of red light.



under irradiation of red left CPL



under irradiation of red right CPL

*Figure 8. germination under red Left and Right circular polarized light*

## References

1. Abe, H.; Yamamoto, K. T.; Nagatani, A.; Furuya, M. *Plant Cell Physiol*, **1985**, 26, 1387-1399.
2. Ausubel, F. M.; Brent, R. E.; Kingston, D.D.; Moore, J. G.; Seidman, J. A.; Smith, K. *Current protocols in molecular biology*, **1989**, 2.3.1-2.3.3.
3. a) Cosgrove, D. J. *Photomodulation of growth*, **1986**, 341-366.  
b) Mullet, J.E. *Annu Rev Plant Physiol*, **1989**, 39, 475-502.  
c) Chory, J.; Nagpal, P.; Peto, C. A. *Plant Cell*, **1991**, 3, 445-459.  
d). Thompson, W. F.; White, M. J. *Annu Rev Plant Physiol Plant Mol Biol*, **1991**, 42, 423-466.
4. Flint, L. H.; McAlister, E. D. *Smithson. Misc. Collect*, **1935**, 94, 1-11.
5. Borthwick, H. A.; Hendricks, S. B.; Parker, M. W.; Toole, E. H.; Toole, V. K. *Proc. Natl. Acad. Sci. USA*, **1952** 38, 662-666.
6. Shropshire, W.; Jr., Klein, W. H.; Elstad, V. B. *Plant Cell Physiol*, **1961**, 2, 63-69.
7. Cone, J. W.; Kendrick, R. E. *Planta*, **1985**, 163, 43-54.
8. Shinomura, T., Nagatani, A., Chory, J. & Furuya, M. (1994) *Plant Physiol*. 104, 363-371.
9. Casal, J.J.; Candia, A. N.; Sellaro, R. *J Exp Bot*, **2014**, 65, 2835-2845.
10. Reed, J. W.; Elumalai, R. P.; Chory, J. *Genetics*, **1998** 148, 1295-1310.

## **Chapter 3.**

### **Hypocotyl elongation**

### 3.1 Introduction

Light controls diverse processes of plant growth and development has been studied by Mohr and Shropshire<sup>1</sup>. Early physiological and photochemical studies indicated that light responses in photomorphogenesis are divided as a low- or high-energy reactions according to their energy requirements<sup>2</sup>. Then, low-energy reactions induced by short pulses of irradiation with relatively small doses of light were presented into low-fluence responses (LFRs) and a very-low-fluence responses (VLFRs) studied earlier by Blaauw<sup>3</sup>, 1968. Phytochrome was first discovered as the photoreceptor for reversibility by red (R) and far-red (FR) light<sup>4</sup>, which was only observed in LFRs. The phytochrome-deficient mutants demonstrated that phytochromes are photoreceptors for VLFR<sup>5</sup> and HIR<sup>6</sup>, although R/FR light reversibility was not observed in either response.

Dark-grown seedlings exhibit etiolated growth, characterized by long hypocotyls, small and closed cotyledons with undifferentiated chloroplasts, and the repression of light-regulated genes<sup>7</sup>. During photomorphogenesis, light inhibits hypocotyl growth (Fig. 1) and promotes cotyledon opening and expansion, chloroplast differentiation and the activation of light-regulated genes. Absorption of red light converts this photoreceptor into a Pfr active form that is translocated into the nucleus<sup>8</sup>, Pfr interacts there with members of the bHLH family of phytochrome-interacting factors (PIFs), involved in modulation of light-regulated genes with a role in photomorphogenesis<sup>9</sup>.

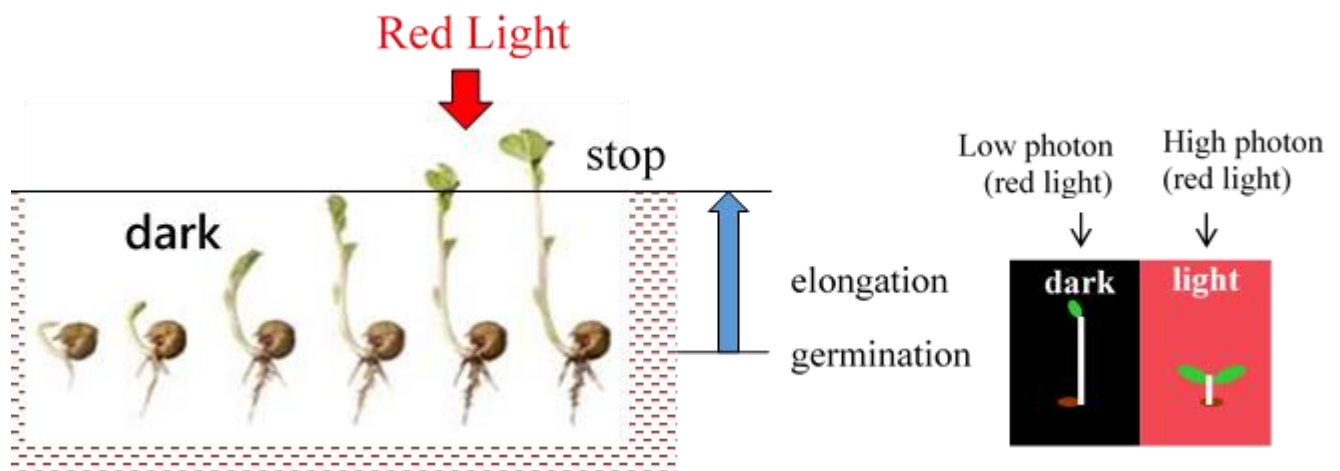
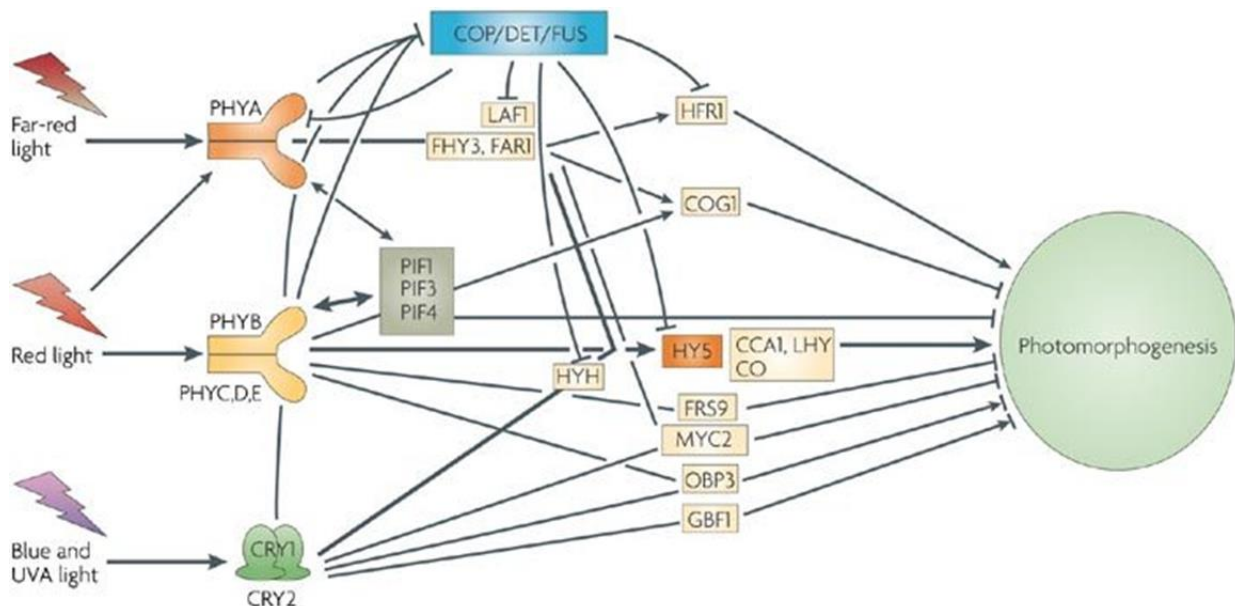


Figure 1. Hypocotyl elongation procedure.

Several transcription factors, which include both positive and negative regulators, have been genetically identified as acting downstream of specific photoreceptors or sets of photoreceptors in photomorphogenesis. Although some transcription factors predominantly respond to one type of light, others respond to two or more. Genetic and genomic analyses suggest the existence of several signalling pathways downstream of PHYA in photomorphogenesis<sup>10</sup> (Fig. 2). Far-red impaired response 1 (FAR1) and Far-red Hypocotyl elongated 3 (FHY3) are both novel transposon-derived putative transcription factors, which interact with each other and are specific to far-red light<sup>11</sup>.



*Figure 2 | Transcriptional networks for seedling photomorphogenesis. A simplified overview of the network involved in this process is shown. Key regulators of this light-regulated transcriptional network have been identified in *Arabidopsis thaliana*, and suggest the existence of separate intermediate networks that are dedicated to each photoreceptor group. A group of PIF transcription factors interact directly with phytochromes and function mainly as repressors of photomorphogenesis. Key transcription factors, such as HY5, serve as signal integration points of major branches downstream of all photoreceptors. The COP/DET/FUS class of factors act as light-inactivatable repressors of photomorphogenesis. Bold lines indicate the convergence pathway.*



The positive function of the PIF4 and PIF5 factors in activated expression of cell elongation genes. In the light, phyB negatively regulates PIF4 transcriptional activity, by targeting degradation of this transcription factor by the 26S proteasome pathway (Fig. 4c). DELLAs repress transcriptional activity of the PIF factors by interacting with the bHLH DNA-recognition domain and sequestering these factors into an inactive complex, unable to bind DNA<sup>12</sup> (Fig. 3).

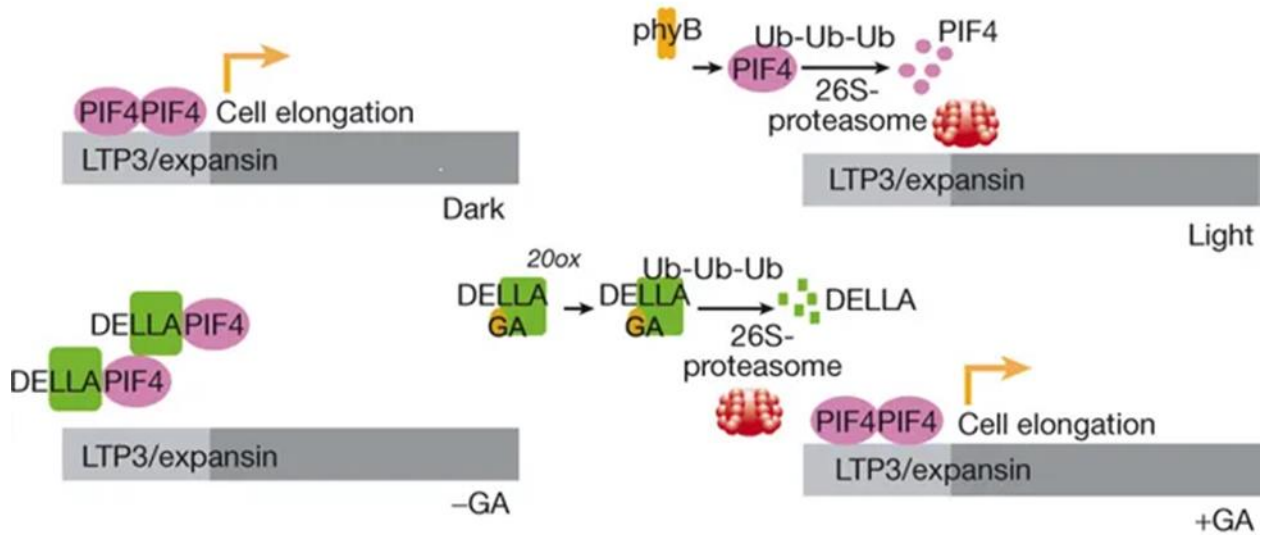


Figure 3: PHYB-mediated degradation of PIF4

### 3.2 Experimental section

#### 3.2.1 materials

Seeds of *Arabidopsis* (*Arabidopsis thaliana*: *At*) wild type (ecotype Columbia-0) and its phyB deficient mutant (*phyB*) were the kind gifts of Prof. Akira Nagatani at Kyoto University. Lettuce seeds (*Lactuca sativa* L.) were purchased from Sakata Seed Corporation (Yokohama, Japan). Surface-sterilized seeds were placed on filter paper soaked with water or Murashige and Skoog (MS) medium supplemented with 2% (W/V) sucrose (Germination Inducible Medium: GIM) in a Petri dish. The seeds were incubated in the dark at 4°C for 48 h to synchronize germination. The detailed growth conditions are shown in each section.

#### 3.2.2 General methods, Instrumentation and measurements

##### *Hypocotyl elongation assay*

Germinated wild type (Ler-0) and *phyB* mutant *Arabidopsis* seeds (20 grains) on water-soaked filter paper in Petri dishes were irradiated with unpolarized white light ( $10.87\mu\text{mol}/\text{m}^2/\text{s}$ ) for 8 h at 22°C. The seeds were cultured under continuous red L- or R-CPL ( $1.02\mu\text{mol}/\text{m}^2/\text{s}$ ) irradiation for 7 or 10 days at 22°C, and the shoots were harvested. Germinated lettuce seeds (20 grains) were cultured and the shoots harvested using the same protocol, except for the omission of white light irradiation. Harvested shoots were photographed, and their hypocotyl lengths were quantified using ImageJ computer software (<https://imagej.nih.gov/ij/download.html>) and compared by Student's t-tests (Fig. 4).

##### Procedure

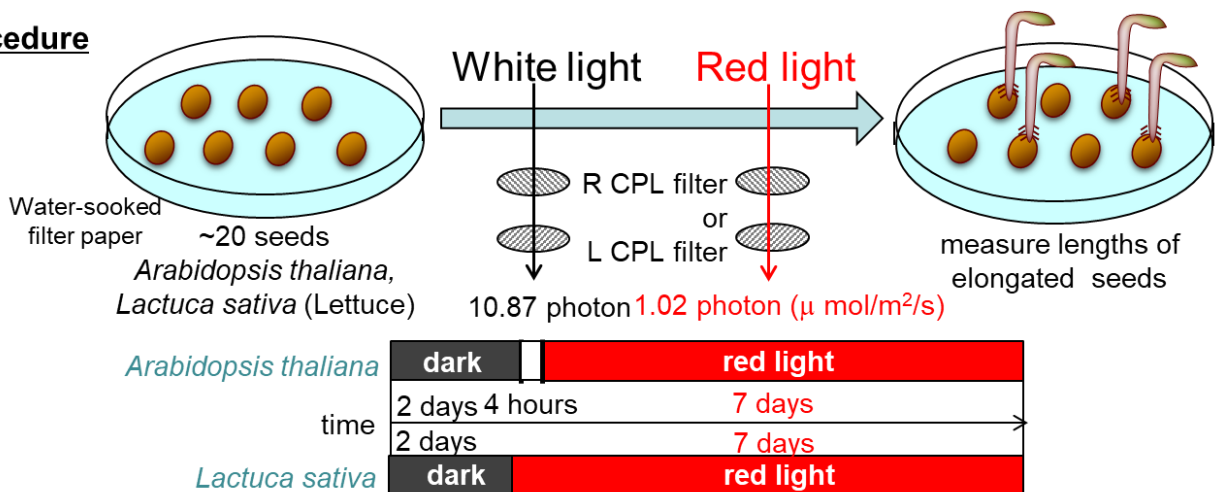


Figure 4. Hypocotyl elongation procedure

### 3.3 Results and discussion

#### Effect of red CPL on hypocotyl elongation of Arabidopsis and lettuce

Assessment of the effects of red CPL on hypocotyl elongation of Arabidopsis showed that the average hypocotyl lengths under L- and R-CPL were 6.4 mm and 5.4 mm, respectively, for 7-day-old seedlings and 7.2 mm and 6.0 mm, respectively, for 10-day-old seedlings (Figure 5A). Similarly, the average hypocotyl lengths of 7-day-old lettuce seedlings under L- and R-CPL were 27.2 mm and 23.0 mm, respectively (Figure 5B). Calculations showed that the hypocotyls of 7- and 10-day-old Arabidopsis seedlings and of 7-day-old lettuce seedlings were 1.18-, 1.20- and 1.18-fold longer, respectively, under L-CPL than under R-CPL.

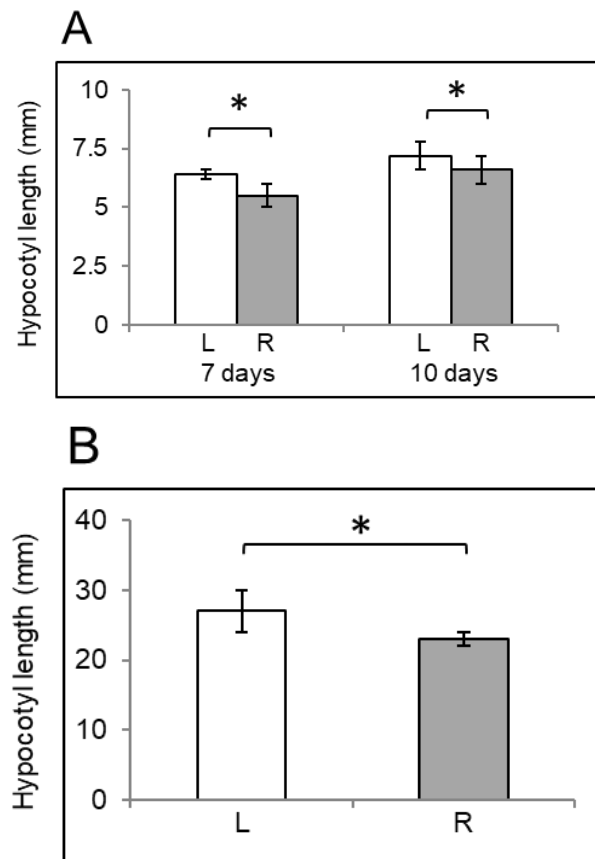
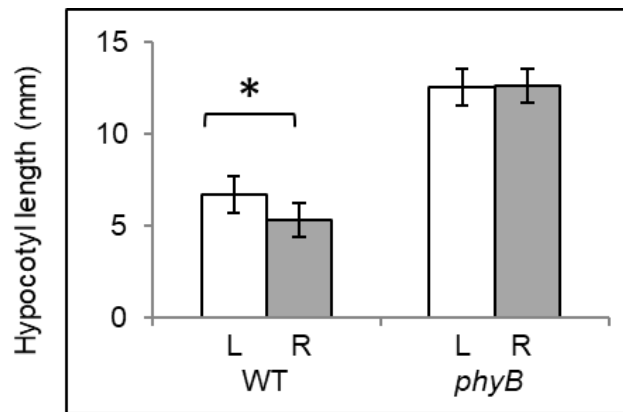


Figure 5. Effect of red CPL on hypocotyl elongation of Arabidopsis (A) and Lettuce (B).

Germinated seeds were cultured in the growth chamber under continuous red L- or R-CPL (white L or grey R column, respectively) for 7 or 10 days (A) and 7 days (B) at 22°C. Then, the seedlings were cut and the hypocotyl length was measured. \*t-test  $P < 0.05$  in each experiment, error bar = S.D.,  $n = 5$ .

### ***Effect of red CPL on hypocotyl elongation of the phyB-deficient mutant of Arabidopsis***

The involvement of phyB in the red CPL effect on hypocotyl elongation was assessed by measuring hypocotyl lengths in a phyB-deficient mutant of Arabidopsis (phyB) grown under L-CPL and R-CPL. The average hypocotyl lengths of 7-day-old wild-type seedlings under L-CPL and R-CPL were 6.7 mm and 5.3 mm, similar to the results in Fig. 6A. In contrast, hypocotyls of the phyB mutant were longer than those of wild-type under both L- and R-CPL, being 12.5 mm and 12.6 mm, respectively, and were almost equal (Figure 6), suggesting that phyB is involved in the red CPL effect on hypocotyl elongation.



*Figure 6. Effect of red CPL on the hypocotyl elongation of Arabidopsis wild type (left WT) and phyB deficient mutant (right, phyB).*

Germinated seeds were cultured in the growth chamber under continuous red L- or R-CPL (white L or grey R column, respectively) for 7 days at 22°C. Then, the seedlings were cut and the hypocotyl length was measured. \*t-test  $P < 0.05$  (left and right), error bar = S.D.,  $n = 4$ .

Hypocotyl elongation of wild-type Arabidopsis was effectively inhibited under R-CPL than L-CPL (Fig. 7). Because this difference was not observed in phyB, it was likely due to light reception by phyB. Hypocotyl elongation in plant seedlings is inhibited by red light perceived by phyB (Reed et al. 1993). The shorter hypocotyl length under R-CPL than under L-CPL was therefore likely due to the phyB-mediated photoinhibition of elongation. Shoots of lentils and peas have been shown to grow faster under L- than under R-CPL<sup>13</sup>. Moreover, the birefringence

of the outer layer of leaves (epidermis) and stems had a negligible effect on light polarization, suggesting that photoreceptors contribute to light perception. Because hypocotyls length was measured in 7-day-old seedlings, the faster growth under L-CPL than under R-CPL may be due to a greater photoinhibition of hypocotyl elongation by R-CPL perceived by phyB. All these results<sup>6,13</sup>, as well as our findings, suggest that phyB is involved in the differential effects of L- and R-CPL on seed germination and hypocotyl elongation.



*Figure 7. hypocotyl elongation under L-CPL and R-CPL.*

## References

1. Mohr, H.; Schopfer, P. *Plant Physiol*, **1995**, 345-373.
2. Mohr, H. *Annu Rev Plant Physiol*, **1962**, 13, 462-488.
3. Blaauw, O. H.; Blaauw-Jansen, G.; Van Leeuwen, W. J. *Avena Planta*, **1968**, 82, 87-104
4. Butler, V. A. V.; Crathorn, A. R.; Hunter, G. D. *Biochem. J.*, **1958**, 69, 544-553.
5. Borthwick, H. A.; Hendricks, S. B.; Parker, M. W.; Toole, E. H.; Toole, V. K. *Proc. Natl. Acad. Sci. USA*, **1952** 38, 662-666.
6. Shinomura, T.; Nagatani, A.; Hanzawa, H.; Kubota, M.; Watanabe, M.; Furuya, M. *Proc Natl Acad Sci USA*, **1996**, 93: 8129- 8133.
7. Chen, M.; Chory, J.; Fankhauser, C. *Annu. Rev. Genet.* **2004**, 38, 87–117.
8. a) Nagy, F.; Schafer, E. *Curr. Opin. Plant Biol.* **2000**, 3, 450–454.  
b) Huq, E.; Al-Sady, B.; Quail, P. H. *Plant J.* **2003**, 35, 660–664.
9. Quail, P. H. *Curr. Opin. Cell Biol.* **2002**, 14, 180–188.
10. a) Wang, H. *Plant J.* **2002**, 32, 723–733.  
b) McCormac, A. C.; Terry, M. J. *Plant J.* **2002**, 32, 549–559.
11. Yuling, J.; On, S.,L.; Xing, W. D. *Nature Reviews Genetics*, **2007**, 8, 217–230.
12. Miguel, L.; Jean-Michel, D.; Mariana, R.; Mariela, P.; Juan, M. I.; Séverine, L.; Christian, F.; Miguel, A. B.; Elena, T.; Salomé, P. *Nature*, **2008**, 451, 480–484.
13. Shibayev, P. C.; Pergolizzi, R. G. *Int J Botany*, **2011**, 7, 113-117.

## **Chapter 4.**

### **Biomass**

## 4.1 Introduction

Efficient use of solar energy for photosynthesis is important for plant growth and survival, especially in low light environments. Plants use light not only as an energy source for photosynthesis but also as an environmental signal and respond to its intensity, wavelength, and direction. Light is perceived by plant photoreceptors such as phytochromes, cryptochromes, and phototropins, and plants generate a wide range of specific physiological responses through these receptors.

In *Arabidopsis thaliana* (Fig. 1), at least 10 photoreceptors, including five phytochromes (phyA through phyE), three cryptochromes (cry1, cry2, and cry3), and two phototropins (phot1 and phot2), have been identified<sup>1</sup>. Phytochromes that absorb red/far-red light and cryptochromes that sense UV-A/blue light coordinately regulate photomorphogenetic processes, including deetiolation, vegetative growth, flowering induction, and circadian rhythms<sup>2</sup>. Phytochrome also regulates seed germination and shade avoidance. By contrast, phototropins that absorb UV-A/blue light have been suggested to play an important role in photo-induced movement responses<sup>3</sup>.

A phototropin was first cloned as a blue light receptor responsible for phototropic bending, using an *Arabidopsis* mutant impaired in phototropism<sup>4</sup>. The mutants lacked light-dependent phosphorylation of a 120-kD protein that appeared related to phototropism. The action spectrum of in vivo phosphorylation of this protein and the fluence dependency of the phosphorylation were similar to those of physiological phototropic responses.

Using an *Arabidopsis* mutant impaired in chloroplast movement, phot2 has been demonstrated to be responsible for the strong-light avoidance response<sup>5</sup>. Moreover, phot2 also is responsible for phototropic curvature in response to relatively high intensities of blue light<sup>6</sup>. Using the *Arabidopsis phot1 phot2* double mutant, it has been demonstrated that phot1 and phot2 redundantly mediate stomatal opening; the blue light-dependent H<sup>+</sup>-pumping activity that drives stomatal opening is lost in the guard cells of mutant plants<sup>7</sup>. More recently, both phot1 and phot2 have been suggested to mediate leaf expansion<sup>8</sup>, and phot1 has been implied to be involved in the rapid inhibition of hypocotyl growth<sup>9</sup>. In contrast with this growth inhibition that is specifically mediated by phot1, genetic studies have revealed that phot1 and phot2 have partially overlapping functions in mediating phototropism, chloroplast movements, stomatal opening, and



leaf expansion<sup>3,5,6</sup>. phot1 seems to be more sensitive to blue light than phot2 in triggering these responses, although sufficient documentation is yet to be provided for leaf expansion.

Provision of an end-of-day(EOD) FR pulse, that rapidly converts Pfr to Pr, has been used extensively as an experimental tool to reduce the persistence of Pfr in darkness<sup>10</sup>. EOD FR treatments initiate the shade avoidance syndrome, which includes responses such as enhanced organ elongation, leaf hyponasty, reduced apical dominance and early flowering<sup>11</sup>. While phyB–phyE operate as R/FR reversible switches, phyA, is functionally distinct, signalling in response to very low fluence rate light or continuous FR irradiation at higher fluence rates, to control a range of responses including germination, seedling de-etiolation and flowering time<sup>12</sup>. Central to light signalling are the phytochrome interacting factors (PIFs) which constitute a clade of the large family of basic helix-loop-helix (bHLH) transcription factors. In the nucleus, light-activated phytochromes interact with and trigger the phosphorylation, ubiquitination and proteasome-mediated degradation of several PIFs<sup>13</sup>.



*Figure 1. Arabidopsis thaliane*

## 4.2 Experimental section

### 4.2.1 Materials

Seeds of Arabidopsis (*Arabidopsis thaliana*: At) wild type (ecotype Columbia-0) and its phyB deficient mutant (phyB) were the kind gifts of Prof. Akira Nagatani at Kyoto University. Lettuce seeds (*Lactuca sativa* L.) were purchased from Sakata Seed Corporation (Yokohama, Japan). Surface-sterilized seeds were placed on filter paper soaked with water or Murashige and Skoog (MS) medium supplemented with 2% (W/V) sucrose (Germination Inducible Medium: GIM) in a Petri dish. The seeds were incubated in the dark at 4°C for 48 h to synchronize germination. The detailed growth conditions are shown in each section.

### 4.2.2 General methods, Instrumentation and measurements

#### *Biomass assay*

Approximately 12 Arabidopsis seeds germinated on GIM-soaked filter paper in Petri dishes were planted in vermiculite soil in a plastic box (40 mm × 33 mm × 15 mm). The plants were grown under unpolarized white light (22  $\mu\text{mol}/\text{m}^2/\text{s}$ ) with a 16 h light/8 h dark cycle for 2 weeks in a cultivation room set at 22°C and ca. 50% humidity.

Seedlings with leaves of similar size were selected, transferred to the growth chamber, and cultured under white L-CPL or R-CPL (10.8  $\mu\text{mol}/\text{m}^2/\text{s}$ ) with a 16 h light/8 h dark cycle for 2 weeks at 22°C. The effect of light quality was measured by turning on one of the LEDs (red, green or blue) in the growth chamber during CPL illumination. Because the fluence rates of the red, green, and blue LED illuminators differed, being 29.7  $\mu\text{mol}/\text{m}^2/\text{s}$ , 5.0  $\mu\text{mol}/\text{m}^2/\text{s}$  and 2.3  $\mu\text{mol}/\text{m}^2/\text{s}$ , respectively, the culture periods were varied, 3 weeks for irradiation with the red and blue LEDs, and 4 weeks for irradiation with the green LED.

The total fluences for the red, green and blue CPL cultures were 35.6, 8.1 and 2.8 mol photons, respectively. The shoots were subsequently harvested and weighed. Biomass was quantified as the average fresh weight per above-ground part of an adult plant and compared by Student's t-tests (Fig. 2).

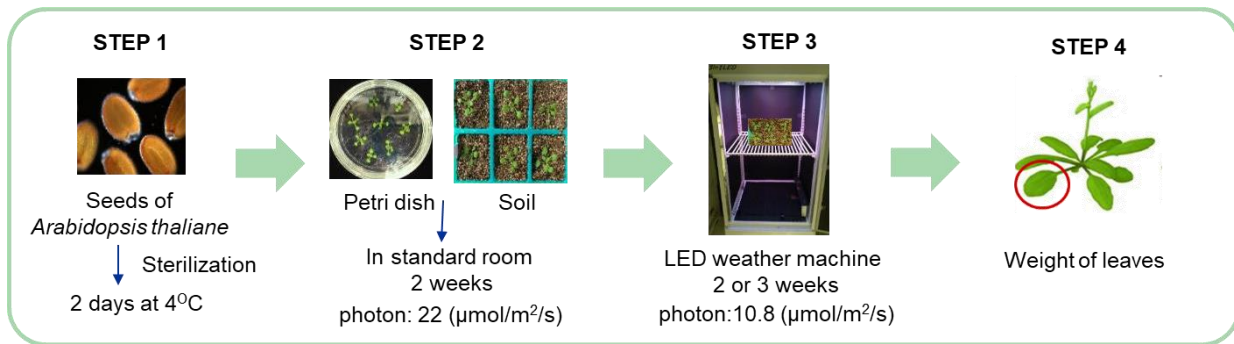


Figure 2. Biomass assay scheme.

## 4.3 Results and Discussion

### *Effect of CPL on biomass production by Arabidopsis*

Evaluation of the effects of white (red + green + blue) CPL on biomass production by *Arabidopsis*, with biomass is defined as the average fresh weight of an above-ground part of an adult plant, found that the average tissue weights L- and R-CPL were 243 mg and 322 mg, respectively, indicating that white R-CPL produced a 1.26-fold greater biomass than white L-CPL (Figure 3A).

To assess the effects of light, *Arabidopsis* was cultured under red, green or blue CPL, although the total fluence of these CPLs differed.

The biomasses produced under red (334 mg vs. 285 mg) and blue (74 mg vs. 58 mg) R-CPL were greater than those produced under L-CPL, ratios of 1.17 and 1.27, respectively. In contrast, green CPL had little effect on biomass production, being 198 mg and 199 mg for green L- and R-CPL, respectively (Figure 3B).

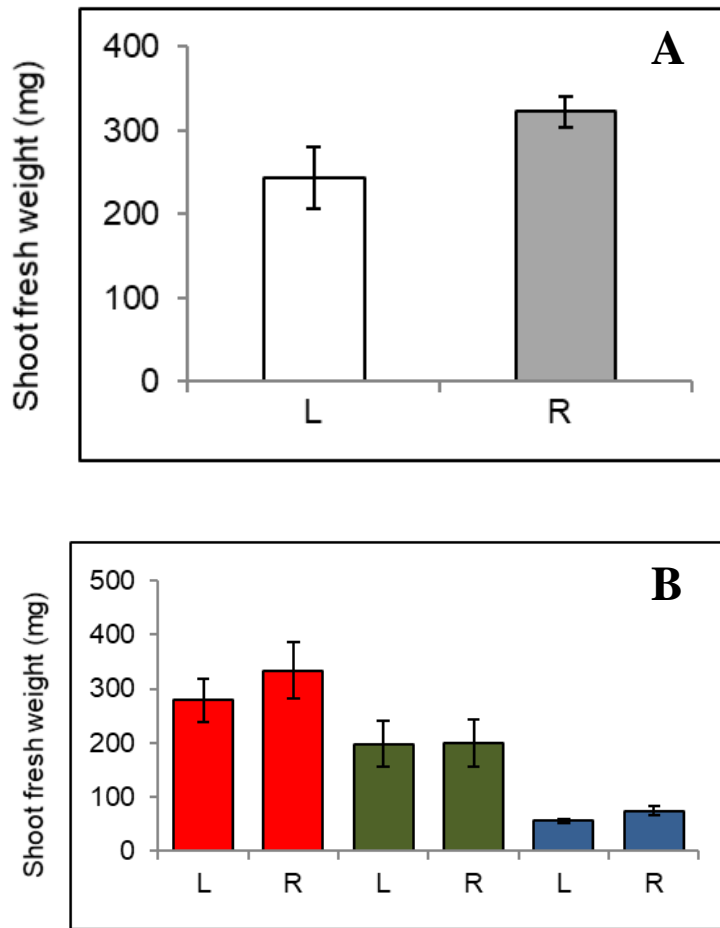


Figure 3. Effect of white CPL (A) and red, green and blue CPL (B) on biomass production by Arabidopsis.

(A) Seedlings planted in soil were cultured under unpolarized white light for 2 weeks with a 16 h light/8 h dark cycle ( $22 \mu\text{mol}/\text{m}^2/\text{s}$ ) at  $22^\circ\text{C}$ . The seedlings were subsequently cultured under white L- (L) or R- (R) CPL with a 16h light/8 h dark cycle at  $10.8 \mu\text{mol}/\text{m}^2/\text{s}$  for 3 weeks at  $22^\circ\text{C}$ . Shoots of the adult plants were cut and their fresh weights were measured.  $P < 0.07$  by t-test, error bar = S.D.,  $N=3$ . (B) Arabidopsis plants were grown under unpolarized white light for 2 weeks, as described in the legend to (A). The plants were subsequently grown under red ( $29.7 \mu\text{mol}/\text{m}^2/\text{s}$  for 2 weeks), green ( $5.0 \mu\text{mol}/\text{m}^2/\text{s}$  for 3 weeks) and blue ( $2.3 \mu\text{mol}/\text{m}^2/\text{s}$  for 3 weeks) L- (L) and R- (R) CPLs, at total fluences of 35.6, 8.1 and 2.8 mol photons, respectively. Shoots of the adult plants were cut and their fresh weights were measured.  $P = 0.128, 0.941$  and  $0.332$  for red, green and blue light, respectively, by t-tests, error bar = S.D.,  $N = 3$ .

### ***Effect of CPL on biomass production***

Understanding the effects of CPL on biomass production may provide useful information to increase crop production in plant factories and may help resolve food crises. Biomass differed markedly in adult green *Arabidopsis* plants grown under L- and R-CPL. Many factors control fresh weight of shoots. The growth and development of plants are regulated by environmental light signals received by photoreceptors. Differences in the effects of L- and R-CPL in blue and red light-absorbing regions suggest the involvement of blue light receptors, such as cry or phot, in addition to phy.

Phot is known to increase the biomass of *Arabidopsis*. The fresh weight of wild type *Arabidopsis* was about three times higher than that of the *phot1/phot2* double mutant under red and weak blue light. This difference was likely due to the role of phot in controlling the opening of the stomata<sup>14</sup> and chloroplast accumulation<sup>15</sup>, which optimize photosynthetic efficiency. Phot has two light, oxygen, and voltage-sensing domains (LOV), LOV1 and LOV2, which bind a flavin mononucleotide (FMN) non-covalently and show a cyclic photoreaction, including transient adduct formation with a nearby cysteine residue<sup>16</sup>. Of the two LOV domains, LOV2 play a major role in regulating physiological responses. FMN of LOV2 in the ground state showed a negative CD in the blue light-absorbing region<sup>17</sup>, indicating that the isoalloxazine ring of FMN exists in an asymmetric environment in protein, compared with a symmetric environment in solution<sup>18</sup>. Taken together, these findings indicate that phot may contribute partly to the larger biomass production under white L-CPL than under white R-CPL.

Phy has been shown to regulate physiological responses in plants, including de-etiolation, shade avoidance and flowering<sup>19</sup>. Cry shows similar regulatory capacity under blue light conditions<sup>20</sup>. Regulation modes related to biomass production differ depending on the growth stage of plant and the light conditions. For example, phyB and cry1 repress hypocotyls elongation in young plants<sup>20</sup>, which may reduce the weight of shoots. However, the perception of light by these photoreceptors increased biomass production in adult tissues<sup>21</sup>. In its ground (oxidized) form, flavin adenine dinucleotide (FAD), the chromophore in cry, also showed a negative CD in the blue light-absorbing region<sup>22</sup>, but showed little CD in solution<sup>23</sup>, similar to FMN of phot. These findings suggest that phyB and cry1 may contribute to the larger biomass production in adult plant under white L-CPL than under white R-CPL.

In addition to light perception by photoreceptors, photosynthesis itself may be involved. L-CPL has shown greater net photosynthesis than R-CPL in a marine alga, *Dunaliella*<sup>24</sup>, a finding consistent with the present results on biomass production. However, no concrete evidence to date has shown that L-CPL induces greater photosynthetic activity than R-CPL in higher plants although many studies have used CD<sup>25</sup> or circularly polarized luminescence<sup>26</sup> Hall et al. 2016), the emission analog of CD, to evaluate the molecular structures and functions of isolated or reconstituted photosynthetic apparatus, such as light-harvesting complexes and reaction centers. These papers reported that the photosynthetic apparatus of these plants was organized chirally, suggesting the need for additional studies to clarify the contribution of photosynthesis to biomass production.

## References

1. Arabidopsis Genome Initiative. *Nature*, **2000**, 408, 796–815.
2. a) Smith, H. *Nature*, **2000**, 407, 585–591.  
b) Lin, C. *Plant Cell*, **2002**, 14, 207–225.  
c) Morelli, G.; Ruberti, I. *Trends Plant Sci*, 2002, 7, 399–403.  
d) Wang, H.; Deng, X.W. *In The Arabidopsis Book*, **2002**, doi/10.1199/ tab.0074, <http://www.aspb.org/publications/arabidopsis/>
3. Briggs, W. R.; Christie, J. M. *Trends Plant Sci*, 2002, 7, 204–210.
4. Huala, E.; Oeller, P. W.; Liscum, E.; Han, I. S.; Larsen, E. Briggs, W. R. *Science*, **1997**, 278, 2120–2123.
5. a) Jarillo, J. A.; Gabrys, H.; Capel, J.; Alonso, J. M.; Ecker, J. R.; Cashmore, A. R. *Nature* **2001**, 410, 952–954.  
b) Kagawa, T.; Sakai, T.; Suetsugu, N.; Oikawa, K.; Ishiguro, S.; Kato, T.; Tabata, S.; Okada, K.; Wada, M. *Science* **2001**, 291, 2138–2141.  
c) Kasahara, M.; Kagawa, T.; Oikawa, K.; Suetsugu, N.; Miyao, M.; Wada, M. *Nature* **2002**, 420, 829–832.
6. Sakai, T.; Kagawa, T.; Kasahara, M.; Swartz, T. E.; Christie, J. M.; Briggs, W. R.; Wada, M.; Okada, K. *Proc. Natl. Acad. Sci. USA*, **2001**, 98, 6969–6974.
7. a) Kinoshita, T.; Shimazaki, K. *EMBO J*, **1999**, 18, 5548–5558.  
b) Doi, M.; Shigenaga, A.; Emi, T.; Kinoshita, T.; Shimazaki, K. *J. Exp. Bot*, **2004**, 55, 517–523.
8. Sakamoto, K.; Briggs, W. R. *Plant Cell*, **2002**, 14, 1723–1735.
9. Folta, K. M.; Spalding, E. P. *Plant J*, **2001**, 26, 471–478.
10. Franklin, K. A.; Whitelam, G. C. *Ann. Bot.* **2005**, 96, 169–175.
11. Franklin, K.A. *New Phytol.* **2008**, 179, 930–944.
12. a) Nagatani, A.; Reed, J. W. Chory, J. *PlantPhysiol*, **1993**, 102, 269–277.  
b) Parks, B. M.; Quail, P. H. *Plant Cell*, **1993**, 5, 39–48.  
c) Reed, J. W.; Nagatani, A.; Elich, T. D.; Fagan, M.; Chory, J. *Plant Physiol*, **1994**, 104, 1139–1149.  
d) Botto, J. F.; Sanchez, R. A.; Whitelam, G. C.; Casal, J. J. *Plant Physiol*, **1996**, 110, 439–444.

- e) Sharrock, R. A.; Clack, T. *Plant Physiol*, **2002**, 130, 442–456.
- f) Shinomura, T.; Uchida, K.; Furuya, M. *Plant Physiol*, **2000**, 122, 147–156
13. a) Ni, M.; Tepperman, J. M.; Quail, P. H. *Cell*, **1998**, 95, 657–667.
- b) Ni, M.; Tepperman, J. M.; Quail, P. H. *Nature*, **1999**, 400, 781–784.
- c) Huq, E.; Quail, P. H. *EMBO J*, **2002**, 21, 2441–2450.
14. Takemiya, A.; Inoue, S.; Doi, M.; Kinoshita, T.; Shimazakia, K. *The Plant Cell*, **2005**, 17, 1120–1127.
15. Gotoh, E.; Suetsugu, N.; Yamori, W.; Ishishita, K.; Kiyabu, R.; Fukuda, M.; Higa, T.; Shirouchi, B.; Wada, M. *Plant Physiol*, **2018**, 178: 1358-1369.
16. Salomon, M.; Eisenreich, W.; Dürr, H.; Schleicher, E.; Knieb, E.; Massey, V.; Rüdiger, W.; Müller, F.; Bacher, A.; Richter, G. *Proc Natl Acad Sci USA*, **2001**, 98, 12357-12361.
17. Corchnoy, S. B.; Swartz, T. E.; Lewis, J. W.; Szundi, I.; Briggs, W. R.; Bogomolni, R. A. *J Biol Chem*, **2003**, 278, 724-731.
18. Abdurachim, K.; Ellis, H. R. *J Bacteriol*, **2006**, 188, 8153-8159.
19. Franklin, K. A.; Quail, P.H. *J Exp Bot*, **2010**, 61, 11-24.
20. Yu, X.; Liu, H.; Klejnot, J.; Lin, C. *Arabidopsis Book* 8, **2010**, e0135.
21. Foreman, J.; Johansson, H.; Hornitschek, P.; Josse, E. M.; Fankhauser, C.; Halliday, K. J. *Plant J*, **2011**, 65, 441-452.
22. Brazard, J.; Usman, A.; Lacomat, F.; Ley, C.; Martin, M. M.; Plaza, P.; Mony, L.; Heijde, M.; Zabulon, G.; Bowler, C. *J Am Chem Soc*, **2010**, 132, 4935-4945.
23. Miles, D. W.; Urry, D. W. *Biochemistry*, **1968**, 7, 2791-2799.
24. McLeod, G. C. *Limnol Oceanogr*, **1957**, 2, 360-362.
25. Krausz, E.; Cox, N.; Årsköld, S. P. *Photosynth Res*, **2008**, 98, 207-217.
26. a) Gussakovsky, E. E.; Ionov, M. V.; Giller, Y. E.; Ratner, K.; Aripov, T. F.; Shahak, Y. *Photosynth Res*, **2006**, 87, 253-265.
- b) Hall, J.; Renger, T.; Picorel, R.; Krausz, E. *Biochim Biophys Acta*, **2016**, 1857, 115-128.



## **Chapter 5**

### **Circular dichroism**

## 5.1 Introduction

Circular dichroism (CD) is based on the differential absorption of the two light vectors. An advantage of the CD method is its independence of the physical form of the analyte. CD measurements can be conducted in solution, gas phase, solid dispersions, films, gels, liquid crystals and monocrystals. CD measures the difference in the absorbance of chiral samples for left ( $A_L$ ) minus right ( $A_R$ ) circularly polarized light usually in the wavelength range of 180-800 nm.

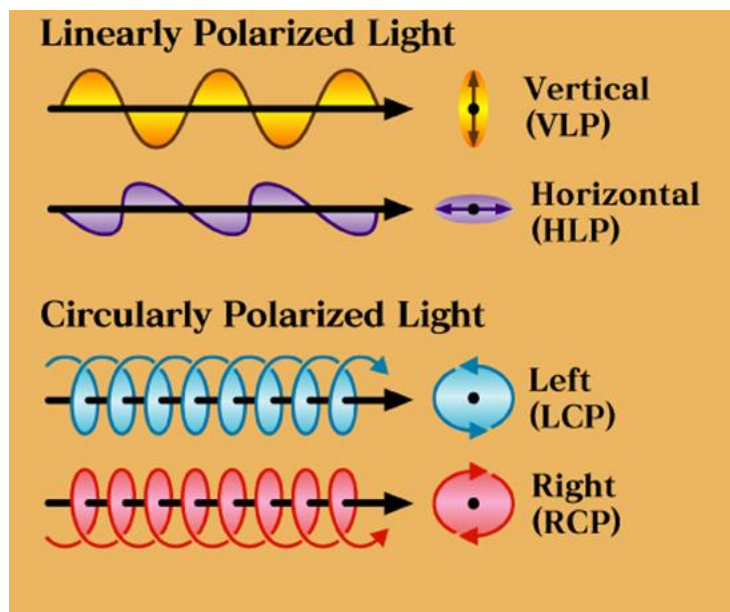


Figure 1. Linearly and Circularly Polarized Lights

$$\Delta A = A_L - A_R$$

This equation,  $\Delta A$  is the directly measured difference of absorbance of left and right polarized light. Assuming the Beer-Lambert's law applies, CD is also presented in terms of the difference in molar absorptivity  $\epsilon$ ,

$$\Delta \epsilon = \epsilon_L - \epsilon_R = \Delta A / cl,$$

Where  $\epsilon_L$  and  $\epsilon_R$  are molar absorption coefficients of left and right handed circularly polarized light, respectively,  $c$  is concentration, and  $l$  is pathlength. In cases where concentration is unknown, it is common to present CD data in ellipticity  $\theta$  (in millideg) or molar ellipticity [M].

$$\theta \text{ (in millideg)} = 32,982 \Delta A$$

$$[M] = 3298 \Delta \epsilon$$

This difference can be detected when a chiral molecule contains one or more light-absorbing groups - so-called chiral chromophores.

When chiral chromophores are present, one state of circularly polarized light will be absorbed to a greater or lesser extent than the other. Over corresponding wavelengths, a circular dichroism signal can, therefore, be positive or negative, depending on whether L-CPL is absorbed to a greater extent than R-CPL (CD signal positive) or to a lesser (Fig. 2) extent (CD signal negative).

The exciton chirality method has dramatically broadened the range of CD applications because its one of the few non-empirical techniques that are capable of determining absolute configuration without the need of any external reference and theoretical calculation.

Recent CD studies have mainly focused on developing chromophores with red shifted and more intense absorption<sup>1</sup> or fluorescence<sup>2</sup>, and intramolecular stacking properties such as porphyrins and zinc porphyrins<sup>3</sup>. CD methods which had obtained the exciton chirality method have been widely used to investigate the configurations and conformations of biomolecules such as nucleic acids<sup>4</sup> and proteins<sup>5</sup>, as well as bioactive natural compounds<sup>6</sup>.

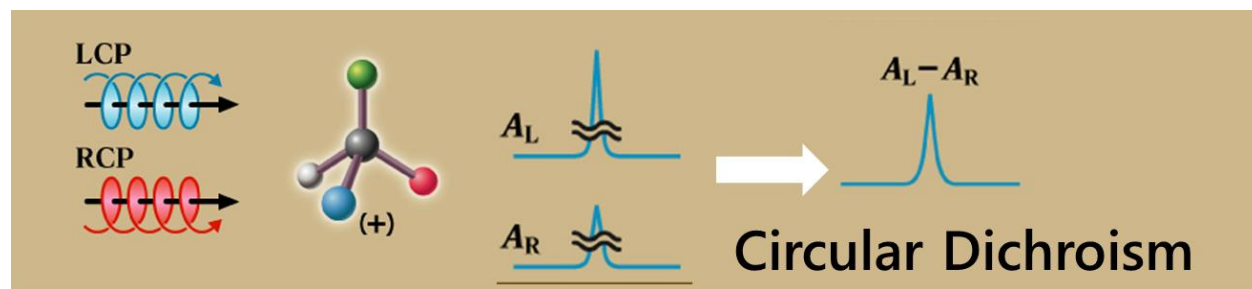


Figure 2. Definition of circular dichroism.

## 5.2 Experimental section

### 5.2.1 Materials

#### *Preparation of PCB-bound AtphyB-N651*

The PCB-bound N-terminal (amino acids 1–651) sensory module of *Arabidopsis thaliana* phyB (AtphyB-N651) was prepared using an *Escherichia coli* (*E. coli*) expression system, essentially

as described<sup>7</sup>. Briefly, *AtphyB-N651* was overexpressed in *E. coli* BL21 (DE3) cells as fusion proteins with the chitin binding domains (CBD) of the PCB synthesizing enzymes HO1 and PCYA from *Synechocystis* sp. PCC6803. The plasmids for the expression of PCB synthesis were the kind gift of Prof. Takayuki Kochi at Kyoto University. The expressed *AtphyB-N651* fused to CBD was purified by chitin affinity chromatography on a prepacked Chitin Beads column (3 ml bed vol. New England Biolabs) according to the manufacturer's instructions, with modifications. The bound protein was washed and self-cleaved by incubating with a cleavage buffer. The eluted sample was purified by ion column chromatography, desalted on a HiTrap Desalting column (GE Healthcare) equilibrated in buffer containing 20 mM Tris-HCl and 0.1 mM Na<sub>2</sub>EDTA, pH 7.8, and applied to a Mono Q 5/50 GL column (GE Healthcare) equilibrated in the same buffer. *AtphyB-N651* was eluted by stepwise application of 0, 100, 200 and 500 mM NaCl in buffer, and by monitoring absorption at 280 nm. Fractions surrounding the elution peak were collected and concentrated on a spin column (Amicon Ultra Centrifugal filter, Millipore).

All procedures were performed at 4°C under dim green safe light. Based on a Coomassie Blue stained SDS- PAGE gel, the purity of the eluted *AtphyB-N651* was estimated to be >95%. Binding of PCB was confirmed at almost 100% by measuring A<sub>650</sub>/A<sub>280</sub> on a UV-Vis absorption spectrophotometer (Figure 3).

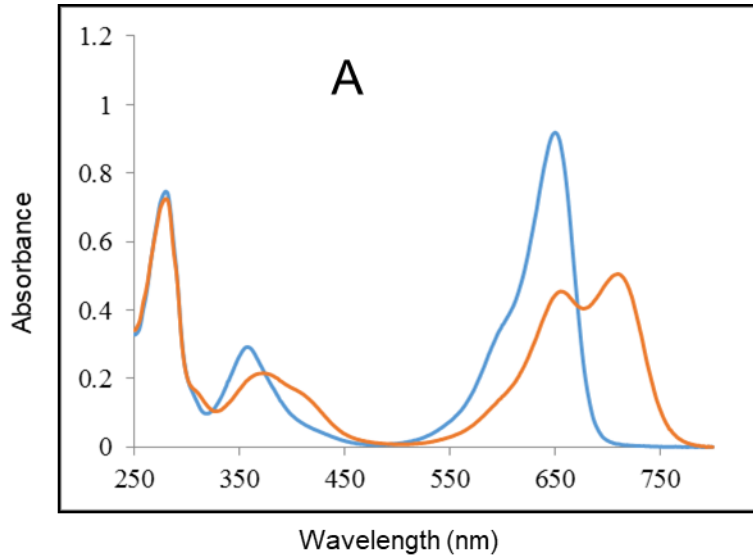


*Figure 3. UV-Vis absorption spectra of PCB-bound AtphyB-N651 in Pr (blue line) and a red light-induced photostationary state (orange line). Spectra of Pr and the red light-induced photostationary state were measured after saturating far-red LPL and under saturating red LPL, respectively, at 25°C*

### ***Spectroscopy***

UV-Vis absorption spectra of AtphyB-N651 in a 25 mM Tris-HCl, pH 7.8 buffer containing 0.5 mM Na<sub>2</sub>EDTA and 125 mM NaCl were recorded at 25°C with a spectrophotometer (model U-3010; Hitachi-Hitec) equipped with a thermostat controller (model 131-0305, Hitachi-Hitec). Samples in the cuvette were illuminated from above at 650 nm for red light and 715 nm for far-red light using an excitation light of a fluorescent spectrophotometer (model RF5300, Shimadzu) guided through a quartz light guide ( $\phi = 1 \text{ cm} \times 1 \text{ m}$ ) and a slit width of 10 nm (Figure 4).

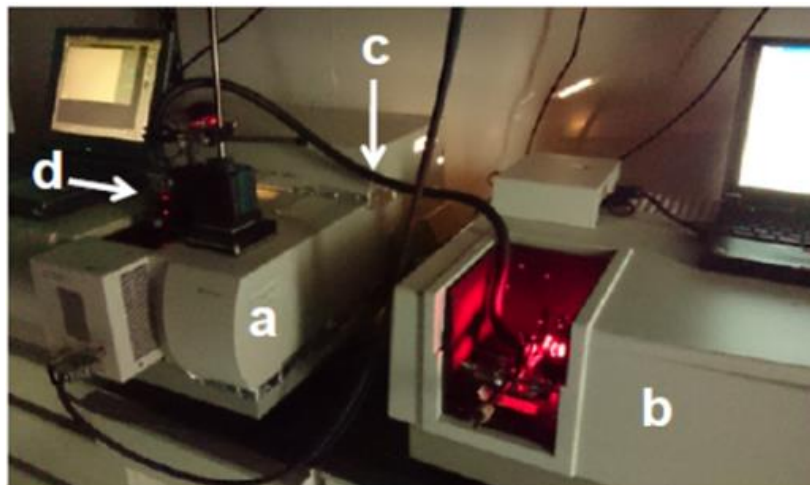


*Figure 4. A picture showing the arrangement of the UV-Vis absorption spectrophotometer (a) and the fluorescence spectrophotometer (b). Excitation light from the fluorescent spectrophotometer is guided to a sample solution in a cuvette set at the cell holder of the spectrophotometer with a quartz light guide (c) from above through a polarized light generator (d).*

The intensity of illumination was adjusted by varying the distance between the end of the light guide and the surface of the sample solution in the cuvette and was measured with a photometric sensor (LI-210R, LI-COR). The effects of polarized light on the photoreaction between Pr and Pfr and the reverse reaction was monitored by repeat scanning of the absorption spectra from 500 to 800 nm at 25°C. LPL, L-CPL and R-CPL were generated by a combination of a polarizer (VIS-NIR high contrast polarizer #47-603, Edmund Optics) and a 1/4 wavelength plate (Achromatic waveplate #65-919, Edmund Optics) (Figure 5).

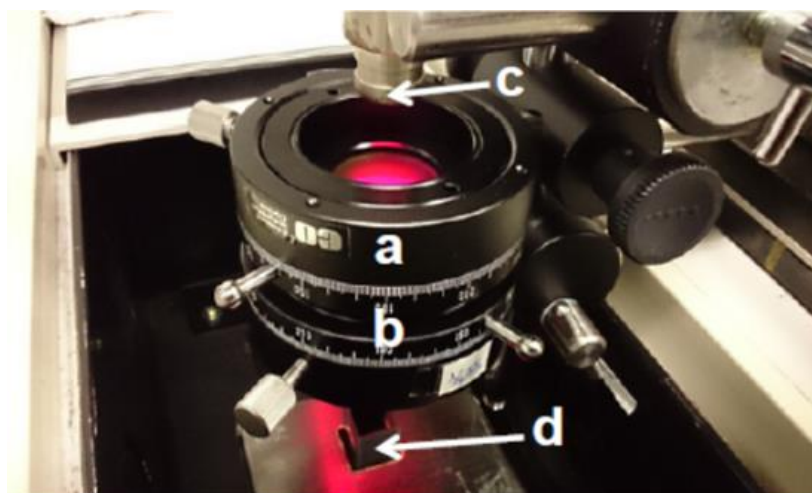


*Figure 5. A picture of the polarized light generator.*

*The generator consists of a polarizer (a) and a 1/4 wavelength plate (b) placed between the light guide end (c) and the surface of a sample solution in a cuvette (d).*

Chiroptical purity and transmittance of the L- or R-CPL were evaluated by a Haze meter (NDH2000, Nippon Denshoku Industries Co., LTD., Japan). No difference between L- and R-CPL was detected (Figure 6).

CD spectra in the UV-Vis absorption region (250–800 nm) were measured at 25°C with a spectropolarimeter (J820, JASCO) equipped with an electric temperature-control system under flowing N<sub>2</sub> gas and an optical path of 1 cm. For each measurement, 10 spectra were collected and averaged. Sample spectra were obtained by subtracting the spectrum of the sample buffer. Before each scan, samples in the cuvette were irradiated with saturating far-red or red light for 3 min to ensure that *A<sub>t</sub>phyB-n651* was in a Pfr or a Pr-induced photostationary state, respectively, because the measuring light of the spectropolarimeter has an actinic effect on the UV-visible absorption spectra of the *A<sub>t</sub>phyB-N651* solutions. To determine the amounts of Pr and Pfr generated by the measuring light of CD, UV-Vis absorption spectra were obtained immediately after the CD measurements. Red and far-red light were supplied from the side of the sample cuvette by the LED illuminators ISL- 150X150-H4FRFR (CCS) and ISL-150X150-H4FRFR (CCS), respectively. Irradiated samples were placed in the sample holder of the spectropolarimeter, and CD scans were started immediately.

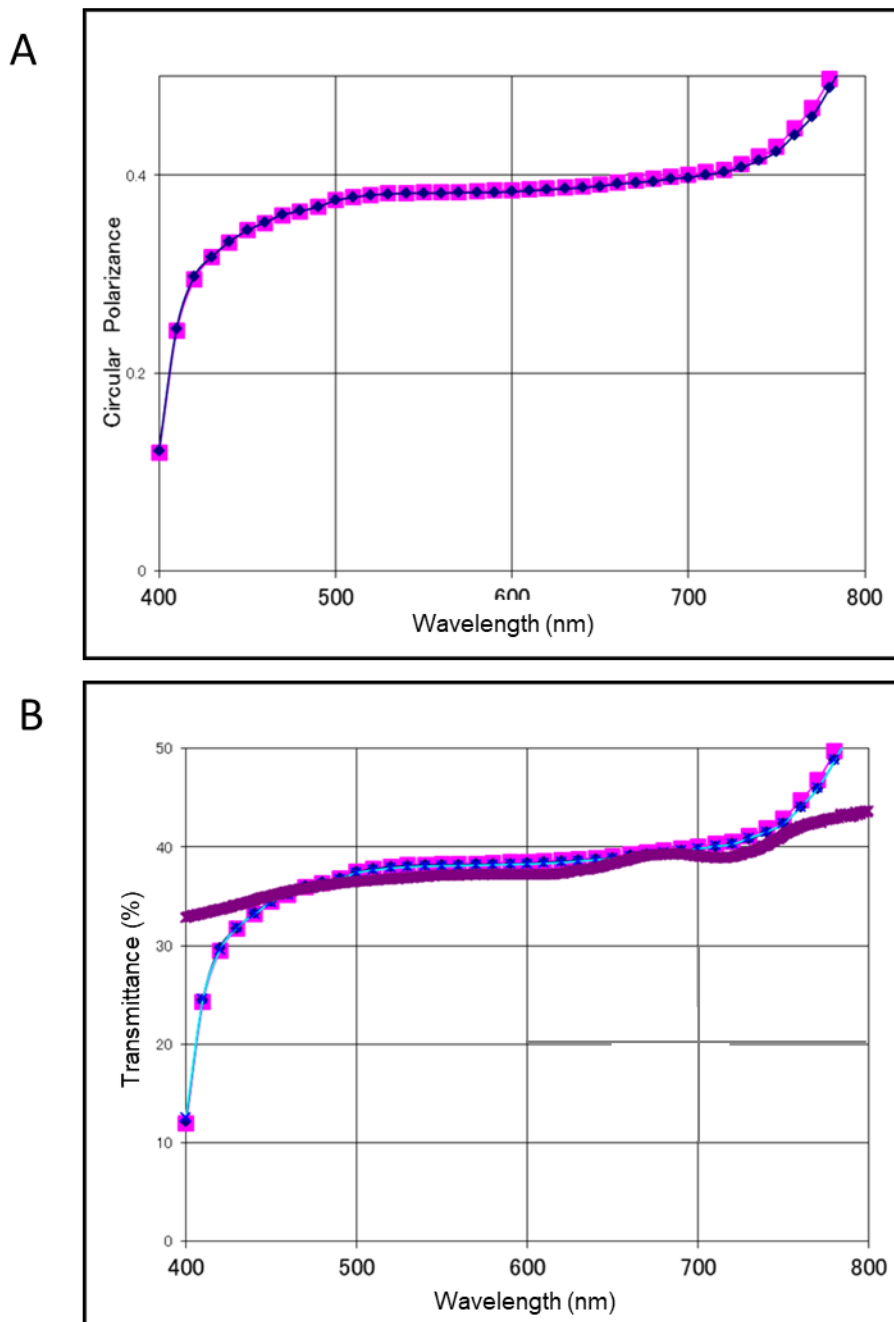


Figure 6. Circular polarization (A) and transmittance (B) of LPL and CPL used for the spectrophotometry. -■-, -◆- and -x- indicate R-CPL, L-CPL and LPL produced by the polarized light generator shown in Supplementary Figure S6. -\* shows the light without polarization.



### 5.3 Results and Discussion

#### *UV-Vis absorption spectra of PCB-bound AtphyB-N651 in Pr and Pfr*

To study the involvement of phyB in the observed effects of CPL, UV-visible (UV-Vis) absorption spectra of a PCB-bound sensory module of Arabidopsis phyB, *AtphyB-N651*, were measured in Pr and a photostationary state between Pr and Pfr induced by saturating with red light illumination (Figure 3). Pfr spectra were constructed by subtracting the Pr spectrum from the spectrum of the photostationary state, so that the shoulder on the Pr spectrum disappears (Figure 8A). The first absorption peaks of Pr and Pfr were at 650 nm and 713 nm, respectively, while their second absorption peaks were at 358 and 372 nm, respectively, with the latter having a shoulder at around 415 nm. These absorption peaks are characteristic of those of PCB-bound cyanobacteria<sup>8</sup> phytochrome 1 (Cph1) and were about 15 nm blue shifted from those of PΦB-bound Arabidopsis phyB27, with the blue shift due to the lack of a one  $\pi$ -electron conjugating system at the edge of the linear tetrapyrrole in PCB (Figure 7).

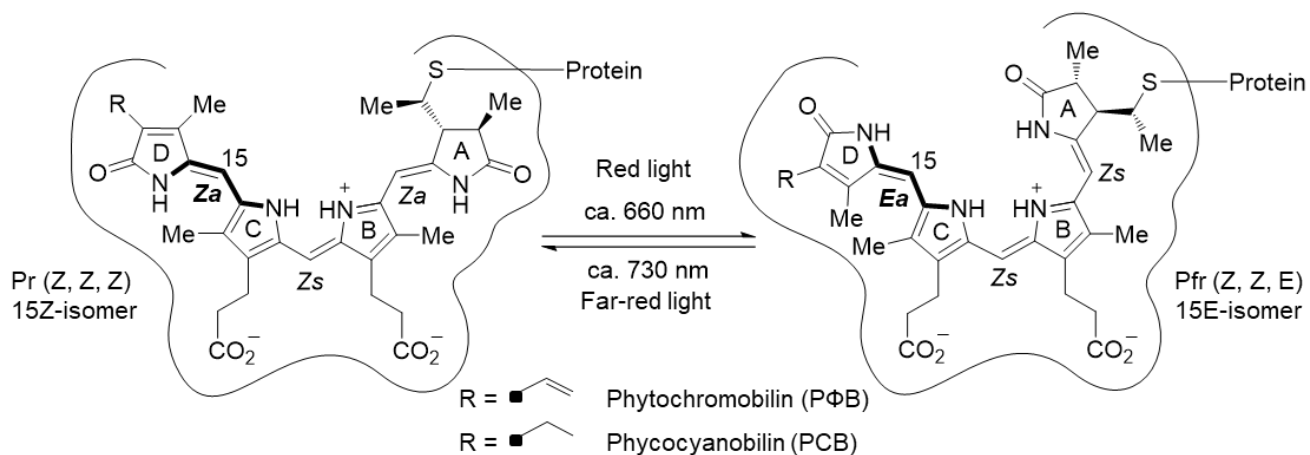


*Figure 7. Schematic illustrations for the structure of a native chromophore phytochromobilin (PΦB) and an analog chromophore, phycocyanobilin (PCB) used in this study in Pr and Pfr. The chromophore undergoes a cis-trans and a reverse photoisomerization at carbon 15 in response to red and far-red light absorption, respectively.*

### *CD spectra of PCB-bound AtphyB-N651 in Pr and Pfr*

CD spectra of PCB-bound AtphyB-N651 were also measured in Pr and a photostationary state between Pr and Pfr induced by saturating with red light illumination (Figure 9). Because of the actinic effect of the strong measuring beam light of CD (see Materials and Methods), the Pr spectrum during CD measurement showed formation of Pfr, as well as a decrease in Pr in the photostationary state.

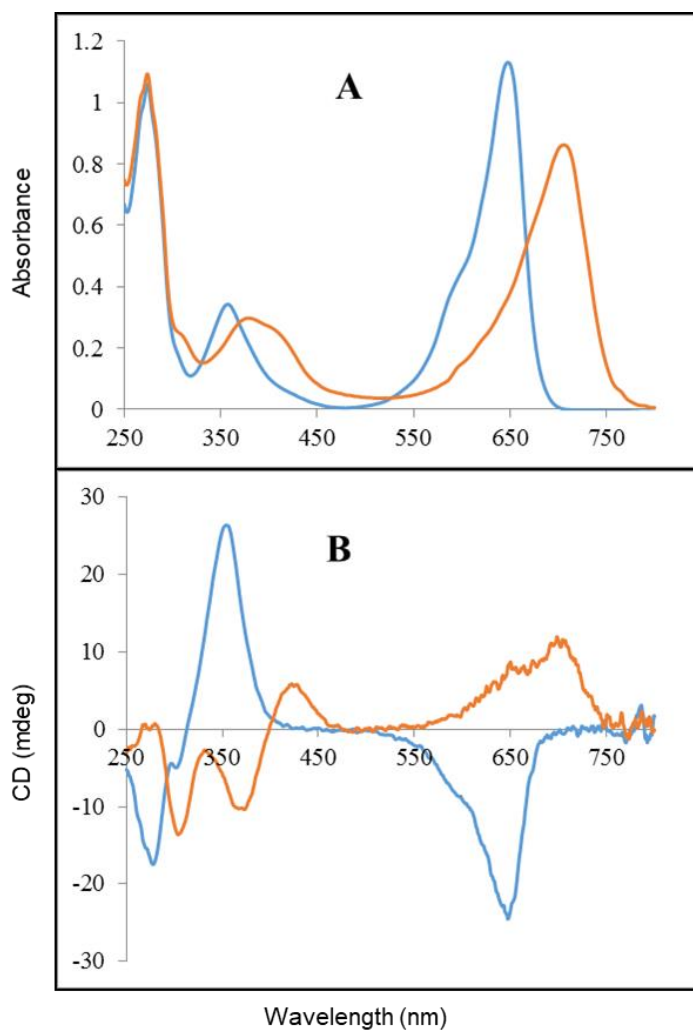


*Figure 8. UV-Vis absorption (A) and CD (B) spectra of AtphyB-N651 in Pr (blue line) and 100% Pfr (orange line). The absorption spectrum of 100% Pfr was calculated from the absorption spectra of Pr and the red light-induced photostationary state shown in Figure 3. CD spectra of 100% Pr and 100% Pfr was calculated from the CD spectra of Pr and a red light-induced photostationary state measured at 25°C (Figure 9) by correcting the actinic effects of the CD measuring light.*

The UV-Vis absorption spectra measured immediately after CD measurements (Supplementary Figure 9A) after illumination with saturating far-red and red light were approximated by superimposition of 89% Pr and 11% Pfr spectra and by 44% Pr and 56% Pfr spectra, respectively (Figure 8). Based on these fractions, the CD (Figure 8B) spectra of 100% Pr and 100% Pfr were constructed from the CD spectra shown in Supplementary Figure 9B.

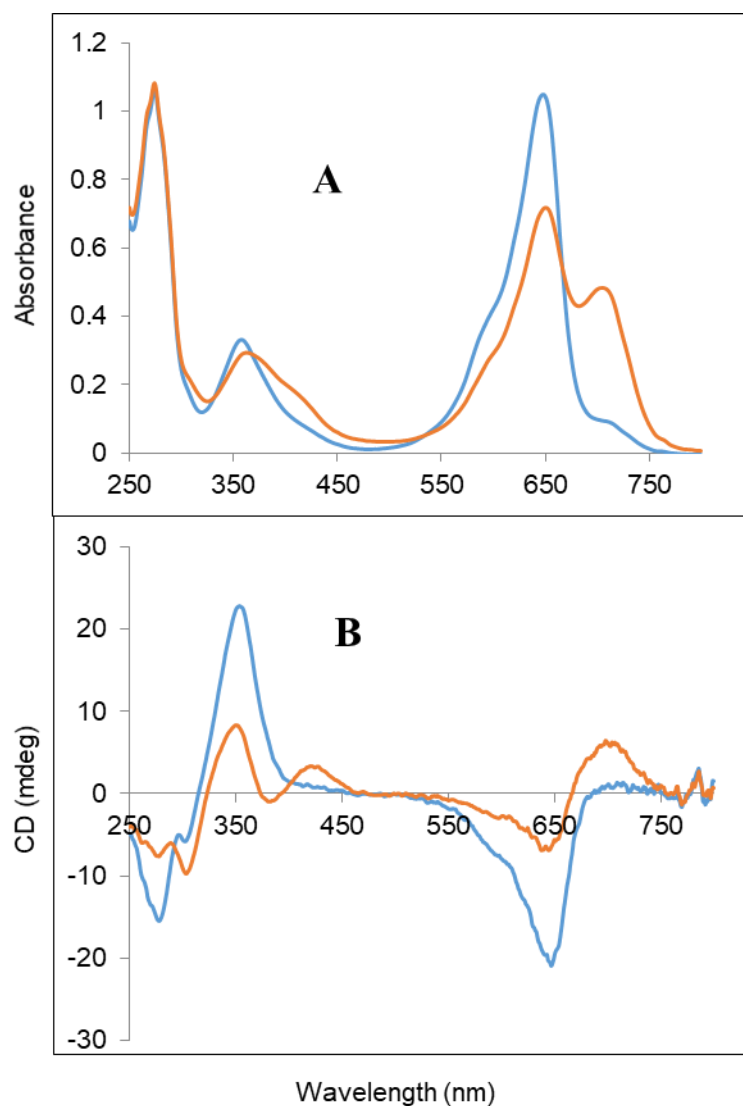


*Figure 9. UV-Vis absorption (A) and CD (B) spectra of PCB-bound AtphyB-N651 measured to calculate CD spectra of 100% Pr and Pfr. CD spectra were measured after saturating far-red (blue) and red (orange line) light irradiation in the same buffer solution as that in Figure 6 at 25°C. UV-Vis absorption spectra were measured immediately after the measurement of the CD spectra to estimate the actinic effect of the CD measuring light.*

The CD spectrum of Pr has negative and positive CD Cotton effects in the regions of the first and second absorption bands, respectively (blue line in Figure 8B), whereas the Pfr CD spectrum of Pfr has a positive Cotton effect in the region of the first absorption band and complex signals in the region of the second absorption band (yellow line in Figure 8B).

### ***Effects of LPL and CPL on the photoreaction of PCB-bound AphyB-N651***

Evaluation of the effects of LPL and CPL on photoreactions from Pr to Pfr (Figure 8) and from Pfr to Pr (Supplementary Figure S3) showed that LPL and both L- and R-CPL induced a reversible phototransformation between Pr and Pfr, similar to that of unpolarized light. These polarizations did not affect the absorption peaks of Pr and Pfr (compare Figure 3 with Figures 10A, B and C and Supplementary Figures S3A, B, and C).

The time courses of the photoreactions from Pr to Pfr (Figures 8D and E) and from Pfr to Pr (Figures 11D and E) monitored at peaks for Pr (650 nm) and Pfr (715 nm) fit well with a single exponential curve of a first-order reaction,  $Abs(t) = A \exp(-kt) + B$  where  $Abs(t)$ ,  $A$ ,  $k$  and  $B$  are absorbance at time  $t$ , a constant of proportionality, a rate constant and an offset, respectively.

Rate constants calculated from the fitting curves are summarized in Table 1. The rate constants for both photoreactions did not differ significantly for L-CPL and R-CPL. In contrast, the rate constants for both photoreactions were slightly higher for LPL than for CPL.

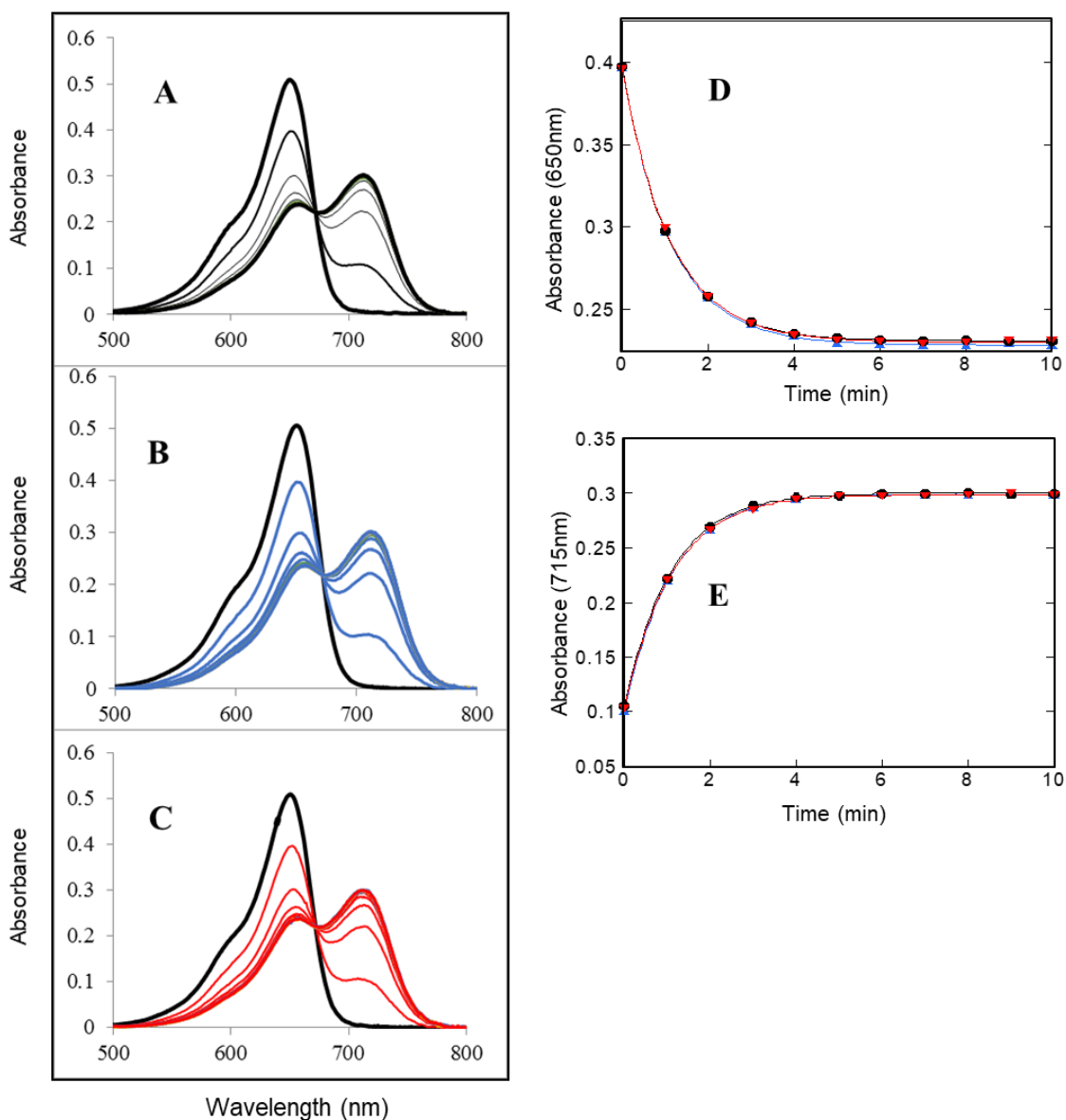


Figure 10. UV-Vis absorption spectra changes of PCB-bound AtpyB-N651 during the photoreaction from Pr to a red light-induced photostationary state at 25°C.

Spectra changes of the Pr (black thick lines) were monitored by repeat scanning of every 1 min (thin lines) until 15 min (thick lines) after the onset of red light illumination of LPL (black lines in A), L-CPL (blue lines in B) and R-CPL (red lines in C). (D) and (E) show kinetics of the photoreaction monitored at a Pr (650 nm) and a Pfr (715 nm) peak, respectively. (●), (▲) and (▼) indicate absorbance changes induced by LPL, L-CPL and R-CPL obtained from the spectra changes in (A), (B) and (C), respectively.

Black, blue and red lines are simulation curves fitted with a single exponential for the first order reaction (see the Results).

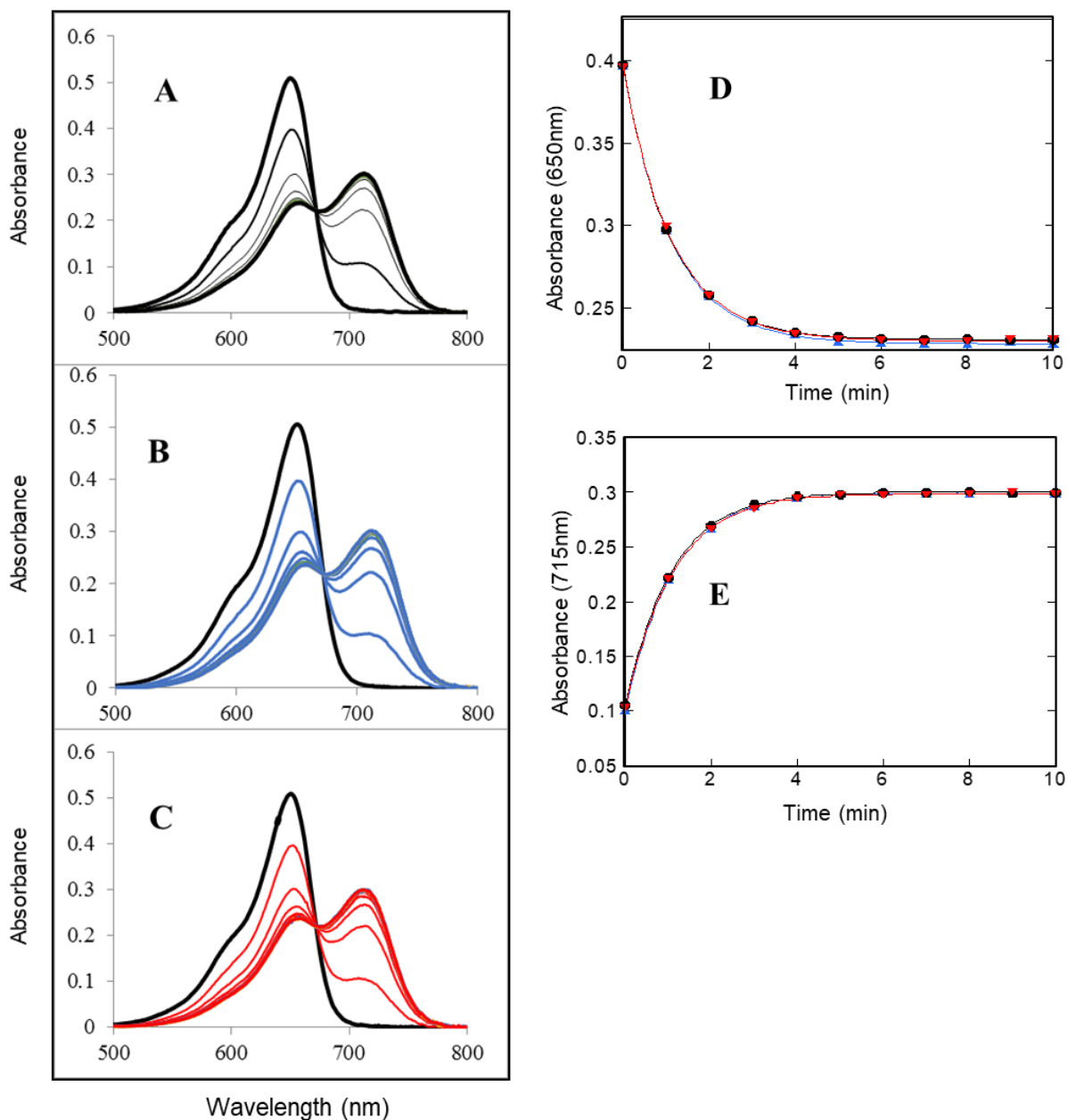


Figure II. UV-Vis absorption spectra changes of PCB-bound AtphyB-N651 during the photoreaction from a red light-induced photostationary state to Pr at 25°C. Spectra changes of the red light-induced photostationary state (black thick lines) were monitored by repeat scanning of every 1 min (thin lines) until 15 min (thick lines) after the onset of far-red light illumination of LPL (black lines in A), L- CPL (blue lines in B) and R-CPL (red lines in C). (D) and (E) show kinetics of the photoreaction monitored at a Pr (650 nm) and a Pfr (715 nm) peak, respectively. (●), (▲) and (▼) indicate absorbance changes induced by LPL, L-CPL and R-CPL obtained from the spectra changes in (A), (B) and (C), respectively. Black, blue and red lines are simulation curves fitted with a single exponential for the first order reaction.

### ***Molecular basis of red CPL perception by phyB***

Phytochromes have been shown to perceive LPL, with red LPL inducing polarotropism in fern and moss protonemata<sup>9</sup>. The transition moments of Pr and Pfr in fern protonemata may be aligned in parallel and normally, respectively, to the cell surface at the periphery of the apical hemisphere. This may be due to localization of phytochrome molecules on the cell membrane surface, with alignment of their molecular axes and directional changes in the moment of transition during phototransformation from Pr to Pfr<sup>10</sup>. The phytochrome involved in this polarotropism was found to be neochrome, a kimeric photoreceptor composed of the N-terminal sensory module of phytochrome and full length phototropin<sup>11</sup>.

A soluble phyB protein, which is present in the cytosol of angiosperms, was shown to be imported into the nucleus upon light activation, forming speckles of as-yet undetermined biological function<sup>12</sup>. Although the orientation of Pfr of phyB in the speckles is not known, Pr of phyB in the cytosol is not oriented. The different responses to red L-CPL and R-CPL must therefore be due to the molecular nature of phyB itself in Pr. The chiroptical spectroscopic properties were therefore evaluated using a PCB-bound sensory module of *At*phyB, consisting of 651 amino acids residues. Crystallographic studies of Pr have revealed a  $5Z_{syn}, 10Z_{syn}, 15Z_{anti}$  configuration for the methylene linkers connecting the four pyrrole rings, both for PCB in Cph1<sup>13</sup> and PΦB in *At*phyB-N90-624<sup>14</sup> (Figure 8). The differences in the effects of red CPL are therefore due to differences in configurations and conformations of the chromophore in Pr of phyB, which is reflected in a CD spectrum. The degree of CD, reported as molar ellipticity  $\theta$ , can be written as  $3300 (\epsilon_L - \epsilon_R)$ , where  $\epsilon_L$  and  $\epsilon_R$  are the molar absorption coefficients of L-CPL and R-CPL, respectively, and a negative CD signal indicates that  $\epsilon_R$  is larger than  $\epsilon_L$ . This is consistent with findings showing that R-CPL generally has greater effects than LCPL. The negative CD signal in the red light-absorbing region may explain, at least in part, the different CPL effects on physiological responses. Upon phototransition from Pr to Pfr, the chromophores of phytochromes isomerize from a  $15Z_{anti}$  to a  $15E_{anti}$  configuration<sup>15</sup>. These conformational changes result in CD spectral changes similar to the CD spectral changes reported with PCB in Cph1<sup>16</sup>.

R-CPL is expected to have a larger effect on  $\epsilon$ , the population of phyB molecules photoconverted from Pr to Pfr, than L-CPL. A larger population of Pfr may result in enhanced

physiological responses and may explain the enhanced germination and stronger photoinhibition of hypocotyl elongation by R-CPL than by L-CPL. However, the contents of Pfr in the red light-induced photostationary state were almost the same for L- and R-CPL. Furthermore, differences in the reaction rates of phototransformation from Pr to Pfr could not be detected, despite R-CPL likely having a greater reaction rate than L-CPL. This may have been due to the limited sensitivity of our optical measurement systems, with minimal detectable changes in absorbance of  $10^{-3}$ . In contrast, the difference between  $\varepsilon_R$  and  $\varepsilon_L$  was of the order  $10^{-6}$ , as the vertical scales of  $\theta$  in the CD spectra are in milli- degrees and  $\theta$  is  $3300 (\varepsilon_L - \varepsilon_R)$ . Thus, the different populations of Pfr in the R-induced photostationary state and differences in the reaction rates of L-CPL and R-CPL could not be detected spectrophotometrically.

### ***Possible amplification of the difference in L- and R-CPL signals***

Despite the very small differences in CD and undetectable absorption spectroscopy, the present results indicate that Arabidopsis can distinguish between R-CPL and L-CPL. Plants as well as animals have various amplification systems for light signals. For example, rhodopsin is highly sensitive and uses well-known biochemical pathways. Carp rhodopsins can induce electrophysiological responses, even when fewer than 1 in  $10^5$  rhodopsin molecules is photoconverted<sup>17</sup>. Plants also have a very highly sensitive response. VLFR can be induced by photoconversion of fewer than 1 in  $10^4$  phyA molecules, a photoreaction too small to be detected with the spectrophotometer used in the present study. Although the signaling networks for VLFR and LFR have been described<sup>18</sup>, the mechanism by which light signals are amplified remains unclear. Known or unknown signal pathways may amplify the small difference in light signals detectable by the CD spectra and undetectable by absorption spectra, resulted in the observed different physiological responses.



## 5.4 References

1. Matile, S.; Berova, N.; Nakanishi, K.; Novkova, S.; Philipova, L.; Blagoev, B. *J. Am. Chem. Soc.* **1995**, 117, 7021-7022.
2. Nehira, T.; Parish, C. A.; Jockusch, S.; Turro, N. J.; Nakanishi, K.; Berova, N. *J. Am. Chem. Soc.* **1999**, 121, 8681-8691.
3. Huang, X.; Fujioka, N.; Pescitelli, G.; Koehn, F. E.; Williamson, R. T.; Nakanishi, K.; Berova, N. *J. Am. Chem. Soc.* **2002**, 124, 10320-10335.
4. a) Johnson, W. C.; In *Circular Dichroism: Principles and Applications*; Berova, N., Nakanishi, K., Woody, R. W., Eds., Wiley-VCH: New York, 2000; 703-718.  
b) Maurizot, J. C. In *Circular Dichroism: Principles and Applications*; Berova, N., Nakanishi, K., Woody, R. W., Eds., Wiley-VCH: New York, 2000; 719-739. c) Ardhhammer, M.; Kurucsev, T.; Norden, B. In *Circular Dichroism: Principles and Applications*; Berova, N., Nakanishi, K., Woody, R. W., Eds., Wiley-VCH: New York, 2000; 741-768. d) Gray, D. M. In *Circular Dichroism: Principles and Applications*; Berova, N., Nakanishi, K., Woody, R. W., Eds., Wiley-VCH: New York, 2000; 769-796.
5. Sreerama, N.; Woody, R. W.; In *Circular Dichroism: Principles and Applications*; Berova, N., Nakanishi, K., Woody, R. W., Eds., Wiley-VCH: New York, 2000; 601-620.
6. Allenmark, S. G. *Nat. Prod. Rep.* **2000**, 17, 145-155.
7. Mukougawa, K.; Kanamoto, H.; Kobayashi, T.; Yokota, A.; Kohchi, T. *FEBS Lett.* **2006**, 580, 1333-1338.
8. Hahn, J.; Strauss, H. M.; Landgraf, F. T.; Gimenez, H. F.; Lochnit, G.; Schmieder, P.; Hughes, J. *FEBS J.* **2006**, 273, 1415-1429.
9. Bünning, E.; Etzold, H. *Ber Dtsch Bot Ges.* **1958**, 71, 304-306.
10. Tokutomi, S.; Mimuro, M. *FEBS Lett.* **1989**, 255, 350-353.
11. Kawai, H.; Kanegae, T.; Christensen, S.; Kiyosue, T.; Sato, Y.; Imaizumi, T.; Kadota, A.; Wada, M. *Nature*, **2003**, 421, 287-290.
12. Nagatani, A. *Curr. Opin. Plant Biol.*, **2004**, 7, 708-711.
13. Essen, L. O.; Mailliet, J.; Hughes, J. *Proc Natl Acad Sci USA*, **2008**, 105, 14709-14714.
14. Burgie, E. S.; Bussell, A. N.; Walker, J. M.; Dubiel, K.; Vierstra, R. D. *Proc Natl Acad Sci USA*, **2014**, 111, 10179-10184.
15. Ulijasz, A. T.; Vierstra, R. D. *Curr Opin Plant Biol*, **2011**, 14, 498-506.

16. Rockwell, N. C.; Shang, L.; Martin, S. S.; Lagarias, J. C. *Proc Natl Acad Sci USA*, **2009**, 106, 6123-6127.
17. Kawamura, S.; Tachibanaki, S. *Comp Biochem Physiol A Mol Integr Physiol*, **2008**, 150, 369-377.
18. Xu, X.; Paik, I.; Zhu, L.; Huq, E. *Trends Plant Sci*, **2015**, 20, 641-650.

## **Chapter 6**

### **Concluding Remarks**

In this thesis, author has conducted the effect of circular polarization light on plant growth, which are germination, hypocotyl elongation and biomass production.

In chapter 2 shows L-CPL and R-CPL have different effects on the germination of Arabidopsis and lettuce seeds. Depending on red light intensity and duration of light illumination studies by circular polarized lights for indicating that the germination rates of Arabidopsis and lettuce induced by red R-CPL were greater than those induced by L-CPL, indicating that the phyB molecules responsible for the seed germination are able to sense the chirality of red light.

In chapter 3 hypocotyl elongation of two different species of photoinhibition by L-CPL and R-CPL and their hypocotyl lengths were quantified using ImageJ computer software. Photoinhibition of hypocotyl elongation of red light perception compared with wild type of seed and mutant type of seeds described. The shorter hypocotyl length under R-CPL than under L-CPL was therefore likely due to the phyB-mediated photoinhibition of elongation. The involvement of phyB in the red CPL effect on hypocotyl elongation was assessed by measuring hypocotyl lengths in a phyB-deficient mutant of Arabidopsis (*phyB*) grown under L-CPL and R-CPL. The average hypocotyl lengths of 7-day-old wild-type seedlings under L-CPL and R-CPL were similar. In contrast, hypocotyls of the *phyB* mutant were longer than those of wild-type under both L- and R-CPL and were almost equal, suggesting that phyB is involved in the red CPL effect on hypocotyl elongation.

In chapter 4, effects of white circular polarized lights on biomass production by Arabidopsis, with biomass is defined as the average fresh weight of an above-ground part of an adult plant, found that the average tissue weights L- and R-CPL. To assess the effects of light, Arabidopsis was cultured under red, green or blue CPL, although the total fluence of these CPLs differed.

The biomasses produced under red and blue R-CPL were greater than those produced under L-CPL, ratios of 1.17 and 1.27, respectively. In contrast, green CPL had little effect on biomass production, for green L- and R-CPL, respectively.

Chapter 5 shows determination of involvement of phyB in the observed effects of CPL, UV-visible (UV-Vis) absorption spectra of a PCB-bound sensory module of Arabidopsis phyB, AtphyB-N651, were measured in Pr and a photostationary state between Pr and Pfr induced by saturating with red light illumination

CD spectra of PCB-bound *At*phtB-N651 were also measured in Pr and a photostationary state between Pr and Pfr induced by saturating with red light illumination. Because of the actinic effect of the strong measuring beam light of CD, the Pr spectrum during CD measurement showed formation of Pfr, as well as a decrease in Pr in the photostationary state. The CD spectrum of Pr has negative and positive CD Cotton effects in the regions of the first and second absorption bands, respectively, whereas the Pfr CD spectrum of Pfr has a positive Cotton effect in the region of the first absorption band and complex signals in the region of the second absorption band.

Evaluation of the effects of LPL and CPL on photoreactions from Pr to Pfr and from Pfr to Pr showed that LPL and both L- and R-CPL induced a reversible phototransformation between Pr and Pfr, similar to that of unpolarized light. These polarizations did not affect the absorption peaks of Pr and Pfr .

## Acknowledgements

I would like to express my deep gratitude to my supervisor Prof. Kenji Monde for past several years, in which he has given valuable opportunities and his excellent guidance.

The author thanks Prof. Junji Yamaguchi and Takeo Sato for many suggestions, useful advices and discussions.

I wish to thank Prof. Kazuhiko Orito for teaching fundamental organic chemistry, reaction mechanism, spectroscopy analyze and pointed appointments. I would like thank Prof. Masaki Anetai for teaching natural product chemistry, spectroscopy analyze and discussions.

Special thanks are given to Osaka Prefecture University for permission experiment, Prof. Satoru Tokutomi for helping research work, Dr. Kazunori Zikihara for lead to CD spectroscopy experiments and discussions. I also would like to thank all member of Fuji Film company. I would like to specially thank Dr. Mitsuyoshi Ichihashi, Mr. Yoshihasi Usami and Takafumi Hosokawa for CPL experiments and good suggestions. I deeply thank to Prof. Tohru Taniguchi, Prof. Yuta Mirai who supporter to my study, Mrs. Yoshiko Sugo and Mrs. Keiko Abe for technical support and encouragement. I am most grateful to thank all my lab colleagues, and I thank to all my friends for longtime friendship.

To my family, Parents D.Lkhamkhuu, Ts. Norovtseren, Parents in law B.Dagvadorj, D.Nyamaa and sister B.Demidkhorloo for their love, support and understanding during the long years education. My deepest thank to my wife D.Ichinkhorloo and our children E.Tselmeg, E.Gerel and E.Mergen for their love and patience. Without her help and encouragement this thesis would not have been completed.

Finally, I would like to thank everybody who was important to the successful realization of thesis as well as expressing my apology that I could not mention personally one by one.